Improvements in clathrate modelling II: the H_2O–CO_2–CH_4–N_2–C_2H_6 fluid system

R. J. BAKKER

Geologisch-Paläontologisches Institut, Universität Heidelberg, Im Neuenheimer Feld 234, D-69120 Heidelberg, Germany

Abstract: Clathrate stability conditions have been modelled for the H_2O–CO_2–CH_4–N_2–C_2H_6 fluid system based on all available experimental data. Optimum Kihara parameters are estimated for pure CO_2, CH_4, N_2 and C_2H_6 gas hydrates from using the most accurate calculation of other parameters involved in clathrate modelling, like fugacities, gas solubilities in H_2O and thermodynamic constants. For mixed gas hydrates of CO_2–CH_4, CH_4–N_2, and CH_4–C_2H_6 excess Gibbs free energy functions are introduced to obtain a good fit to experimental data. The excess Gibbs free energy is described according a modified Margules equation, which depends on mole fraction and temperature.

Gas hydrates are ice-like solids that form part of the clathrate family. They occur regularly in natural rock (e.g. Sloan 1990) and in fluid inclusions in single crystals (e.g. Roedder 1963). Gas hydrates are solid-solutions of H_2O and gases such as CO_2, CH_4, N_2, and C_2H_6, and its stoichiometry depends on temperature and pressure. Knowledge of the stability conditions of this clathrate phase as a function of salinity, temperature and pressure forms the basis of any conclusive predictions in clathrate-related oceanographic and atmospheric studies. Purely empirical best-fits to experimental data are the easiest way for modelling clathrate stability conditions, and this method has been frequently favoured throughout decades of clathrate research (e.g. Deaton & Frost 1946; Bozzo *et al.* 1975; Dholabhai *et al.* 1993). The non-stoichiometry and the infinite compositional combinations of clathrates, however, require a more thorough approach for interpolations and extrapolations of clathrate stability conditions in natural systems. Equilibrium thermodynamics is an important tool for a systematic approach of modelling clathrate melting conditions as a function of composition, temperature, pressure and salinity. Platteeuw & van der Waals (1958) and van der Waals & Platteeuw (1959) were the first to use this approach, which was only possible after thorough studies of the crystallographic structure of the solid clathrate phase by, for example, von Stackelberg & Müller (1954). Platteeuw & van der Waals (1958) and van der Waals & Platteeuw (1959) modified the absorption theory according to Langmuir (1918) to a three-dimensional generalization describing the physical interaction of a captured gas molecule in a cage of H_2O molecules. This model was the first to describe systematically clathrate stability conditions of pure and mixed gas clathrates.

The basic concept of the model from van der Waals & Platteeuw (1959) is the equality of chemical potential of one component in each phase in which it is present, which is the most important prerequisite for any equilibrium thermodynamics:

$$\mu_{H_2O}^{vap} = \mu_{H_2O}^{liq} = \mu_{H_2O}^{clath} \quad (1)$$

where the superscripts indicate the phases (vap is vapour, liq is liquid and clath is clathrate). The chemical potential of H_2O in the clathrate phase is obtained from statistical thermodynamics using the partition functions (van der Waals & Platteeuw 1959):

$$\mu_{H_2O}^{clath} = \mu_{H_2O}^{empty} + RT\sum_i \nu_i \ln\left(1 - \sum_M y_{Mi}\right) \quad (2)$$

where $\mu_{H_2O}^{empty}$ is the chemical potential of a hypothetical gas-free (empty) clathrate, R is the gas constant ($=8.31439\,J\,mol^{-1}\,K^{-1}$), T is temperature in Kelvin, ν_i is the number of cavities of type i per cage forming H_2O molecule and y_{Mi} is the probability of finding a gas molecule M in cavity of type i. van der Waals & Platteeuw (1959) related the probability y_{Mi} to Langmuir constants (equation (3)), which in turn are related to molecular cell potentials (equation (4))

$$y_{Mi} = \frac{C_{Mi} f_M}{1 + \sum_K C_{Ki} f_K} \quad (3)$$

$$C_{Mi} = \frac{4\pi}{kT}\int_0^\infty \exp\left(\frac{-w(r)}{kT}\right) r^2\,dr \quad (4)$$

BAKKER, R. J. 1998. Improvements in clathrate modelling II: the H_2O-CO_2-CH_4-N_2-C_2H_6 fluid system. *In:* HENRIET, J.-P. & MIENERT, J. (eds) *Gas Hydrates: Relevance to World Margin Stability and Climate Change*. Geological Society, London, Special Publications, **137**, 75–105.

where C_{Mi} is the Langmuir constant for gas M in a cavity of type i, f_M is the fugacity of gas M, k is the Boltzman constant, r is the distance to the centre of the cavity and $w(r)$ is the spherically symmetrical potential function describing the intermolecular potential between a gas molecule at the centre of the cage and an H_2O molecule of the cavity wall. Equations (2)–(4) are a combination of Langmuir's isotherm, which is characteristic for localized adsorption without interaction of the adsorbed molecules, and a generalization of Raoult's law for the properties of the solvent in a solution where solute–solute interaction can be neglected.

In the scope of this study it is important to focus on the major postulates originally proposed by van der Waals & Platteeuw (1959), apart from their axiom of classical statistics:

(a) the mode of occupation of the cavities does not affect the contribution of the H_2O molecules to the total chemical potential of the host lattice;
(b) a cavity can never hold more than one encaged molecule, which is always localized in the cavities;
(c) the mutual interaction of the solute molecules is neglected;
(d) the solute molecules can rotate freely in their cavities, i.e. the rotational partition function for the motion in the cavity is the same as that in the perfect gas;
(e) the potential energy of a solute molecule when at a distance r from the centre of its cage is given by the spherically symmetrical potential $w(r)$ proposed by Lennard-Jones & Devonshire (1937, 1938) for dense gases. This method is equally valid for the cavities in a clathrate, as long as one restricts oneself to first neighbour interactions.

By that time, van der Waals & Platteeuw (1959) already indicated the limitations of these postulates. Encaged molecules with larger dimensions, like CO_2, may distort host lattice and damage assumption (a). Postulate (c) can never be strictly true because numerical calculations and experimental evidence show that the contribution of solute–solute interaction to the configurational energy is at most a few per cent of the energy of binding of the solute molecules in their cages. Non-spherical molecules, like O_2 and N_2, will not be free to rotate in the entire cavity. When such a molecule comes close to the wall of its cage it will have to orientate itself parallel to this wall. The relative contribution of second and third neighbour solvent molecules to $w(r)$ in hydrate structures is only of the order of a quarter of that in the much denser face-centred cubic lattice. Despite the indicated limitations of the postulates (a)–(e), van der Waals & Platteeuw (1959) were able to give a clear relation between the equilibrium vapour pressure, composition, and chemical potential of the solvent in a clathrate. The individual postulates (a)–(e) have frequently been modified (e.g. McKoy & Sinanoglu 1963; Saito *et al.* 1964; Parrish & Prausnitz 1972; Ng & Robinson 1976; Holder *et al.* 1980; Dharmawardhama *et al.* 1980; John *et al.* 1985; Munck *et al.* 1988; Dubessy *et al.* 1992; Bakker *et al.* 1996) to increase the physical integrity at molecular scale and to obtain a better fit to increasingly available experimental data.

Modifications proposed by Bakker *et al.* (1996) for pure CO_2 clathrate with various salts are further developed in this study for a complex fluid system including H_2O–CO_2–CH_4–N_2–C_2H_6. The aim of this study is to present a model which is based on all available experimental data within this fluid system, and which is able to reproduce these data accurately over a wide range of TP conditions. In addition, we have tried to avoid increasing the complexity of the model, which has no experimental justification, and to show that some original proposed principles are eminently useful in describing this fluid system accurately.

Topology of H_2O–CO_2–CH_4–N_2–C_2H_6 fluids near clathrate melting conditions

Qualitative thermodynamic equilibria analysis, based on Gibbs phase rule, constrains possible configurations for this multi-component fluid system (Fig. 1). Five phases, i.e. clathrate, water, gas mixtures (liquid- and vapour-like) and ice form the basic ingredients for this analysis. Equilibrium between three phases is illustrated by univariant lines, which intersect at invariant quadruple points Q_1 and Q_2 (e.g. Fig. 1d), where four phases form a stable configuration. Quadruple point Q_2 can only be present if the immiscibility field of gas mixtures and pure gases, i.e. the dew-point curve and bubble-point curve, intersects the limits of the clathrate stability field (Fig. 1c and d). Quadruple point Q_1 remains a point for this multi-component system because the coexisting gas mixture is always vapour-like. Q_2 is transformed in a line segment for ternary and higher-order fluid systems. Clathrate melting conditions for binary gas–H_2O systems are represented by Fig. 1a

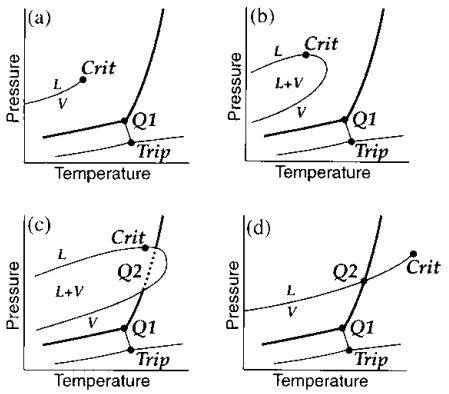

Fig. 1. Schematic $P-T$ diagrams illustrating the position of the clathrate stability field (shaded areas) compared to the position of liquid–vapour equilibria of pure gases, (**a**) and (**d**), and gas mixtures, (**b**) and (**c**). L, liquid; V, vapour; Crit, critical point; Q_1, quadruple point 1; Q_2, quadruple point 2; Trip, triple point of pure H_2O.

and d. These topologies form the basis of the systematic clathrate modelling in this study.

Model modifications

Improvements and simplifications of the clathrate model as proposed by Bakker *et al.* (1996) are further developed for the multi-component H_2O–CO_2–CH_4–N_2–C_2H_6 fluid system.

Thermodynamic properties of H_2O in the liquid phase

The thermodynamic properties of pure H_2O in liquid and solid phase are intensively studied fluid parameters in the literature (e.g. Franks 1972). Several recently published equations of state for pure H_2O (e.g. Haar *et al.* 1984; Hill 1990) are able to describe accurately all measurable properties of this fluid from a unified Helmholtz function, i.e. saturation properties, densities, pressures, speed of sound, specific heats and virial coefficients. In general, these studies do not include metastable regions for the H_2O phase. Although many parameters for H_2O are accurately known, most clathrate stability models include oversimplified values for density and specific heat. For example, constant values have been used for these parameters by, for example, Munck *et al.* (1988) and Dubessy *et al.* (1992). Bakker *et al.* (1996) introduced a more accurate calculation of these parameters, using published equations of state that reproduce accurately experimental data, even extended into metastable regions. The molar volume of liquid H_2O is calculated from the equation of state as proposed by Kell & Whalley (1965) and Kell (1967) up to 100 MPa. At higher pressures, the equation from Haar *et al.* (1984) is used. The heat capacity of liquid H_2O is obtained from Osborne *et al.* (1939). At temperatures below 273.15 K, a polynomal best-fit (Bakker *et al.* 1996, p. 1662, equation 6) was obtained through data on metastable liquid H_2O from Angell *et al.* (1973).

van der Waals & Platteeuw (1959) concentrated on clathrate equilibrium in the presence of pure ice and a gas phase. They did not consider explicitly an equilibrium involving a liquid solution, because solubilities of the solute in the liquid phase should be taken into account. The chemical potential of H_2O in the liquid phase was, in general, not known at that time. The effect of gas solubilities in an ideal liquid solution was introduced by Saito *et al.* (1964) and Parrish & Prausnitz (1972). According to relatively simple thermodynamics, the chemical potential of H_2O in the liquid solution ($\mu^{liq}_{H_2O}$) is defined by:

$$\mu^{liq}_{H_2O} = \mu^{pure}_{H_2O} + RT\ln(a_{H_2O}) \qquad (5)$$

where $\mu^{pure}_{H_2O}$ is the chemical potential of pure H_2O at a selected temperature and pressure, and a_{H_2O} is the activity of H_2O. The activity coefficient for H_2O is assumed to be equal to 1 due to low gas solubilities, and, therefore, activities can be replaced by mole fraction in real solutions. However, the activity coefficient is noticeably affected in salt-bearing solutions and it should, therefore, be obtained from theoretical consideration by Debye & Hückel (1923) and Pitzer (1992) on dissolved electrolytes, as illustrated for some selected liquid solutions by, for example, Englezos & Bishnoi (1988), Dubessy *et al.* (1992) and Bakker *et al.* (1996).

Thermodynamic properties of gas hydrates

To illustrate directly equilibrium conditions for clathrates as a function of Langmuir constants van der Waals & Platteeuw (1959) defined the difference between the chemical potentials of H_2O in the two modifications, i.e. empty clathrate and ice. The quotient of this difference ($\Delta\mu_{H_2O}$) and RT was directly related to measurable parameters such as enthalpy differences and

volume changes:

$$\frac{\Delta\mu_{H_2O}(T,P)}{RT} = \frac{\Delta\mu^{ref}_{H_2O}}{RT_0} - \int_{T_0}^{T}\left[\frac{\Delta h_{H_2O}}{RT^2}\right]dT + \int_{P_0}^{P}\left[\frac{\Delta v_{H_2O}}{RT}\right]dP \quad (6)$$

where $\Delta\mu^{ref}_{H_2O}$ is the chemical potential difference at standard conditions T_0 and P_0, Δh_{H_2O} and Δv_{H_2O} are the difference in enthalpy and molar volume, respectively, which may be obtained from the Clapeyron equation and structural data on crystal lattices. This difference was considered a standard value for a given clathrate structure, because it is not related to the type of encaged gas molecule. The standard value for $\Delta\mu^{ref}_{H_2O}$ could have been obtained from direct analysis of the composition of clathrates at 0°C. However, determination of the composition of clathrate compounds with direct chemical analysis seems to be problematic, and many significantly different values have been published (Sloan 1990, p. 231, table 5-5). Bakker *et al.* (1996) give thorough arguments for the adoption of the values given by Dharmawardhama *et al.* (1980) as standard values at 273.15 K and 0.1 MPa. The standard chemical potentials $\mu^{empty}_{H_2O}(ref)$ and enthalpy $h^{empty}_{H_2O}(ref)$ of the hypothetical empty clathrate Structure I and II (Table 1) are obtained after addition of the standard values for the well-defined thermodynamic constants for the liquid solution or ice to $\Delta\mu^{ref}_{H_2O}$ from equation (6). The standard value for entropy $s^{empty}_{H_2O}(ref)$ is deduced from these values according to classical thermodynamics:

$$\mu^{empty}_{H_2O}(ref) = h^{empty}_{H_2O}(ref) - T_0 \times s^{empty}_{H_2O}(ref) \quad (7)$$

where T_0 is 273.15 K. Equation (6) has been extensively used in literature and it has been built up to extreme proportions. For example, the use of classical thermodynamics for this arbitrarily defined chemical potential difference lead to very complex notations (e.g. Parrish & Prausnitz 1972). A better organization of these formulae improves the survey of the model. In fact, there is no need to use this difference because the values for one component, i.e. ice and water, are well defined in the literature (see previous section). Simplifying thermodynamic notations, Bakker *et al.* (1996) used straightforward thermodynamics to calculated the chemical potential of empty clathrates:

$$\mu^{empty}_{H_2O}(T,P) = \mu^{empty}_{H_2O}(ref) - \int_{T_0}^{T} s^{empty}_{H_2O}\,dT + \int_{P_0}^{P} v^{empty}_{H_2O}\,dP \quad (8)$$

where $s^{empty}_{H_2O}$ and $v^{empty}_{H_2O}$ are entropy and molar volume of the empty clathrate, respectively. In most studies, the temperature and pressure dependency of thermodynamical properties of hypothetical empty clathrates were set equal to some properties of pure ice. In this study, the temperature dependency of entropy is obtained from the heat capacity equation for pure ice (Equation 9), which was fitted to experimental data from Giauque & Stout (1936) between 240 and 270 K (Bakker *et al.* 1996, p. 1661, equation 5). This linear function has to be extrapolated to temperatures well above pure ice melting conditions (up to 320 K) for clathrate stability conditions at higher pressures. Equation (9a) is assumed to be appropriate for both clathrate structures and ice

$$c^{empty}_{P_{H_2O}} = -0.3840 + 0.1406 \times T \quad (9a)$$

$$s^{empty}_{H_2O}(T) = s^{empty}_{H_2O}(ref) + \int_{T_0}^{T}\left(\frac{c_P}{T}\right)dT. \quad (9b)$$

The volumetric properties of the hypothetical empty clathrate are obtained from the so-called equation of state for pure ice. This equation combines the isothermal compressibility (equation (10a)) according to Bakker *et al.* (1996),

Table 1. *Thermodynamic properties of water in four phases at standard conditions of 273.15 K and 0.1 MPa*

Phase	μ_0 (kJ mol^{-1})	h_0 (kJ mol^{-1})	s_0 (J mol^{-1})	v_0 (kJ mol^{-1})
Liquid	−303.935	−286.634	63.34	18.01
Ice	−303.916	−292.645	41.26	19.65
Clathrate Structure I (empty)	−302.638	−291.256	41.67	22.35†
Clathrate Structure II (empty)	−302.961	−291.620	41.52	22.57†

† Avlonitis (1994).

and thermal expansion of clathrate structures I and II (equations (10b) and (10c)) according to Avlonitis (1994). Equation (10) gives, therefore, a complete description of volumetric properties of the empty clathrate structure at selected temperatures and pressures

$$v_P = v_0 \times \exp[-K\Delta P] \quad (10a)$$

$$v_{H_2O}^{\text{empty I}} = v_P(1.0 + 3.1075 \times 10^{-4}\Delta T + 5.9537 \times 10^{-7}\Delta T^2 + 1.3707 \times 10^{-10}\Delta T^3) \quad (10b)$$

$$v_{H_2O}^{\text{empty II}} = v_P(1.0 + 1.9335 \times 10^{-4}\Delta T + 21768 \times 10^{-7}\Delta T^2 - 1.4786 \times 10^{-10}\Delta T^3) \quad (10c)$$

where Roman numerals I and II refer to clathrate Structure I and II, v_0 is the molar volume at reference conditions (Table 1), K is the isothermal compressibility ($=10^{-4}$ MPa), ΔP is the difference between the pressure (in MPa) of interest and the standard pressure (=0.1 MPa), and ΔT is the difference between the temperature (in K) of interest and the standard temperature (=273.15 K).

Clathrate stability predictions appear to be highly sensitive to the size of cavities (e.g. Lundgaard & Mollerup 1992). Most studies have adopted a constant value for the cell radius (R) of spherical symmetrical cavities, and volumetric properties were only used for the chemical potential difference calculations in equation (6). Bakker *et al.* (1996) introduced a variable cell radius which is in a straightforward relation to volumetric properties from equation (10). Changes in molar volume resulting from variable temperature and pressure can be characterized by the total differential of equation (10) (equation (11a)). Isotropic behaviour of the clathrate structure relates the alterations in cavity radius to the cubic root of this changes in molar volume of the clathrate phase (equation (11b))

$$dV = \left(\frac{\partial V}{\partial T}\right)_P dT + \left(\frac{\partial V}{\partial P}\right)_T dP \quad (11a)$$

$$dR \equiv \sqrt[3]{dV}. \quad (11b)$$

Fugacity coefficients of gases

Calculation of gas fugacities is applied to all phases which appear in equation (1). Fugacity coefficients are calculated from equations of state, which describe accurately the relation between P–T–V–X properties of fluids, according to the theoretical considerations from Prausnitz *et al.* (1986). In addition, the accuracy of fugacity calculations is dependent on the ability of equations of state to represent volumetric data for the entire pressure range from 0 MPa to the pressure of interest.

There is a rich supply of equations of state from the literature, and the selection is based, first, on the temperature and pressure of interest to clathrate stability conditions. Secondly, the equation of state should be able to describe CO_2–CH_4–N_2–C_2H_6 mixtures, which also include very small amounts of H_2O. Bakker *et al.* (1996) have demonstrated this selection procedure for pure CO_2 gas hydrates. This selection procedure has been omitted in most other studies.

Recently, unified Helmholtz energy functions have been developed for many pure gases, such as H_2O (Haar *et al.* 1984; Hill 1990), CO_2 (Span & Wagner 1996), CH_4 (Setzmann & Wagner 1991), N_2 (Angus *et al.* 1979) and C_2H_6 (Friend *et al.* 1991). These equations of state accurately describe P–T–V properties of pure gases over a wide range of temperatures and pressures. Unfortunately, these function are only defined for pure components and they are not available for gas mixtures. Therefore, another family of equations of state, such as the modifications to the equation of state according to van der Waals (1873), Benedict *et al.* (1940) or Carnahan & Starling (1969) have to be used in this study. These equations have a limited range of application and should be carefully selected. First, the clathrate melting pressure is described as a polynome in temperature (equation (12) and Table 2), which is fitted to experimental data for pure gas hydrates

$$\log_{10}(P) = A + BT_C + CT_C^2 + DT_C^3 \quad (12)$$

where T_C is temperature in °C, and P is pressure in MPa. Equation (12) is of direct use to pure gas hydrates, and can be applied for the temperature range indicated in Table 2. Along this polynome several equations of state are compared to fugacity calculations for the pure gases (Fig. 2), which are obtained from the previously mentioned unified Helmholtz energy function. Comparison to pure gases is justified because the gas mixture contains in general less than 0.1 mol% H_2O. The equation of states according to Redlich & Kwong (1949), Chueh & Prausnitz (1967), Soave (1972), Lee & Kesler (1975), Holloway (1977, 1981), Flowers (1979) and Duan *et al.* (1992*a*, *b*, 1996) are used for comparison (Fig. 2).

Table 2. *Constants in equation (12) to calculate clathrate stability for pure gas hydrates*

Gas hydrate	A	B	C	D	Temperature interval (°C)
CO_2	0.087925	0.049309	0.00068487	–	−1.5 to 9.9
	−8.3417	1.6697	−0.093782	0.0018506	9.9–20
CH_4	0.43115	0.034	0.0010333	-1.7994×10^{-5}	−0.3 to 40
N_2	1.208	0.046288	−0.00017311	–	−1.3 to 27
C_2H_6	−0.30931	0.046365	0.00072746	–	−0.1 to 14.6
	−8.1526	0.87596	−0.019077	–	14.6–18

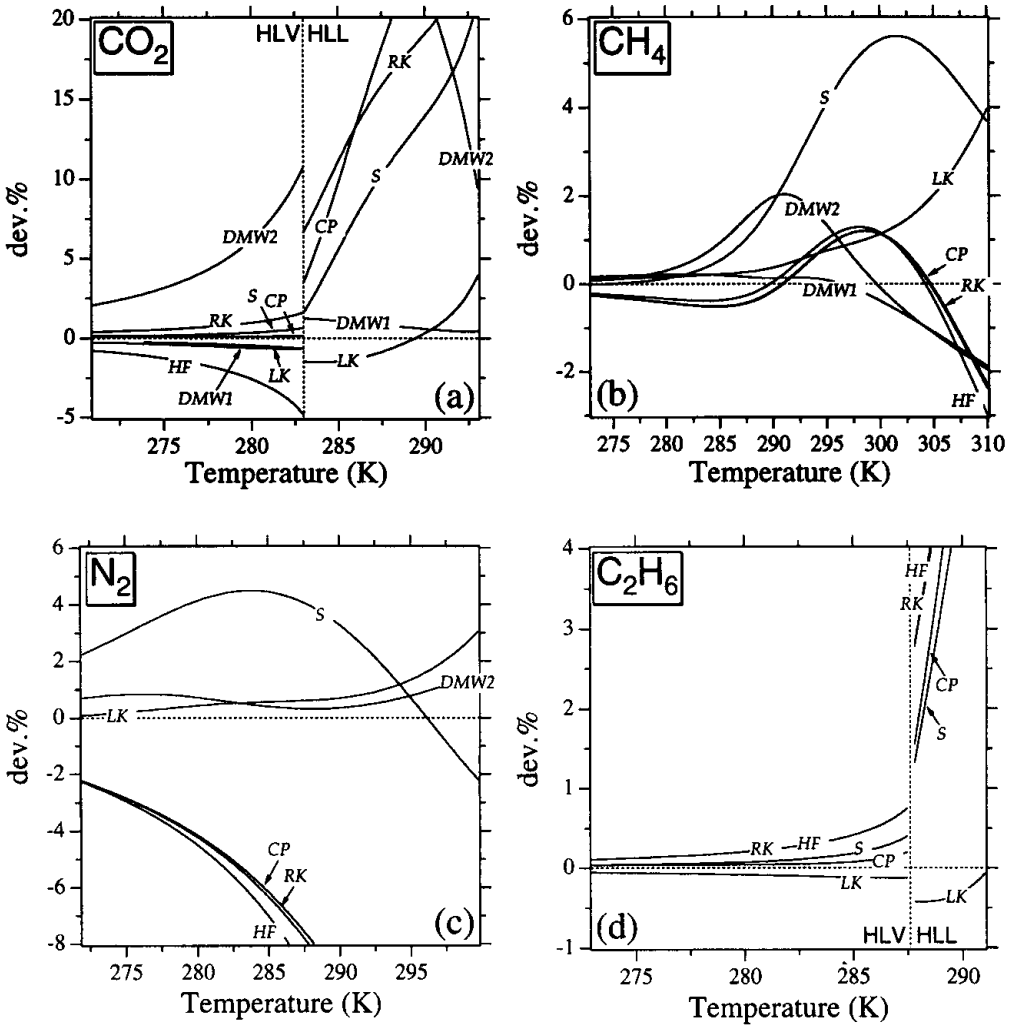

Fig. 2. Comparison of fugacity calculation for pure gases (**a**) CO_2; (**b**) CH_4; (**c**) N_2; (**d**) C_2H_6, obtained from several equations of state (RK, Redlich & Kwong 1949; CP, Chueh & Prausnitz 1967; S, Soave 1972; LK, Lee & Kesler 1975; HF, Holloway 1977, 1981; and Flowers 1979; DMW1, Duan *et al.* 1992*a*, *b*; DMW2, Duan *et al.* 1996), which can be used for gas mixtures including small amounts of H_2O. Deviation (dev.%) is defined as a percentage from fugacities obtained from unified Helmholtz energy functions. The vertical dashed line for CO_2 (**a**) and C_2H_6 (**d**) marks the boundary between clathrate melting in equilibrium with a liquid-like gas-rich phase (HLL) and a vapour-like gas-rich phase (HLV).

Table 3. *Selected equations of state for fugacity calculations at clathrate melting conditions*

Gas	EOS
CO_2	Duan *et al.* (1992*a*, *b*)
CH_4	Duan *et al.* (1992*a*, *b*)
N_2	Duan *et al.* (1996)
C_2H_6	Lee & Kesler (1974)

Table 3 gives selected equations of state which reproduce most accurately the P–T–V–X properties, in particular fugacity, of the fluid at clathrate melting conditions for pure gas hydrates. The equation of state according to Duan *et al.* (1992*a*, *b*) has been chosen for fugacity calculations of pure CO_2 gas hydrate and pure CH_4 gas hydrate. Duan *et al.* (1996) provides the equation of state for pure N_2 gas hydrates, and Lee & Kesler (1975) for C_2H_6. The accuracy in fugacity calculations of these equations remains within 2%.

Solubility of gases

Although the solubility of gases like CH_4 and N_2 in H_2O is very low (e.g. Culberson & McKetta 1951), a small difference in H_2O activity may seriously affect modelled clathrate stability conditions. The solubility of gases can be theoretically predicted with equations of state that accurately describe both coexisting liquid and vapour phases at relative low-temperature conditions (e.g. Lundgaard & Mollerup 1991). This model is based on the equality of chemical potential of all components in each coexistent phase (equation (13)), which are obtained from one equation of state

$$\begin{cases} \mu^{\text{liq}}_{H_2O} = \mu^{\text{vap}}_{H_2O} \\ \mu^{\text{liq}}_{M} = \mu^{\text{vap}}_{M} \end{cases} \tag{13}$$

where subscript M refers to any type of dissolved gas. Some equations of state accurately describe liquid–vapour equilibria for H_2O–free gas mixtures (e.g. Thiéry *et al.* 1994), however, the liquid-like coexisted phase in clathrate stability calculations is H_2O-rich. The previously mentioned equations of state for the fugacity calculation accurately describe only a part of binary H_2O-gas mixtures. For example, the experimental data on CH_4 solubility in H_2O from Culberson & McKetta (1961) are accurately reproduced by Duan *et al.* (1992*a*, *b*). However, the coexisting composition of the vapour phase is increasingly in error at higher temperatures (Fig. 3). Furthermore, the method of liquid–vapour equilibria calculation from a single equation of state is a lengthy operation due to the numerical–iterative approach. Therefore, Henry's law has been used to replace the liquid phase part of equation (13). Henry's law appears to represent more accurately the low solubility data of gases in H_2O at temperature-pressure conditions relevant to clathrate stability con-

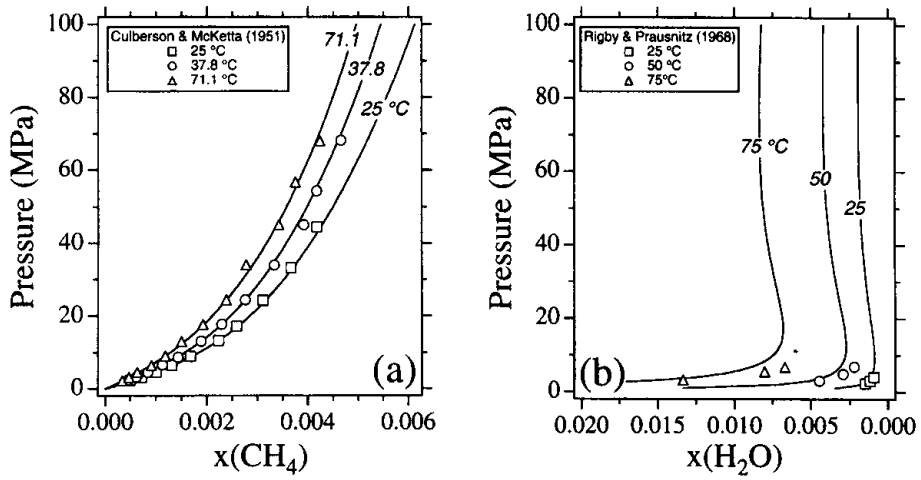

Fig. 3. P–X diagrams for comparison of solubility data of (**a**) CH_4 in H_2O liquid from Culberson & McKetta (1951) and (**b**) H_2O in CH_4 vapour from Rigby & Prausnitz (1968) to calculated coexisting liquid and vapour compositions from the equation of state according to Duan *et al.* (1992*a*, *b*) at selected temperatures.

ditions. Bakker *et al.* (1996) illustrated the careful choice of the equation according to Carroll *et al.* (1991) and Carroll & Mather (1992) for the CO_2 solubility in H_2O. Using a similar approach, Henry's constants of CH_4 and C_2H_6 from Rettich *et al.* (1981), and of N_2 from Benson & Kraus (1976), are chosen to calculate their solubility in H_2O. A polynome in reciprocal temperature is the general form to describe the temperature dependence of these Henry's constants:

$$\ln(H) = a_0 + \frac{a_1}{T} + \frac{a_2}{T^2} + \frac{a_3}{T^3} + \frac{a_4}{T^4} \qquad (14)$$

where H is Henry's constant in MPa, and a_i are the coefficients for individual gases (Table 4). It is important to realize that Henry's constants are directly related to gas fugacities according to equation (13), and the originally measured mole fraction of gas in solutions can only be reproduced exactly if a similar equation of state is used to calculated fugacities of components in the vapour phase. Fortunately, fugacity calculations from different equations of state do not differ significantly at these relatively low-temperature conditions. At higher pressures, adjustments of Henry's constant are described according to the correction from Krichevsky & Kasarnowsky (1935):

$$\ln(H)_P = \ln(H)_{P_{ref}} + \int_{P_{ref}}^{P} \left(\frac{v^{\infty}_{gas}}{RT}\right) dP \qquad (15)$$

where v^{∞}_{gas} is the partial molar volume of a gas at infinite dilution (Table 4), and equation (14) is used to calculate Henry's constants at the reference pressure of 1 atmosphere.

Intermolecular potential

Platteeuw & van der Waals (1958) and van der Waals & Platteeuw (1959) used the cell theory according to Lennard-Jones & Devonshire (1937, 1938) to describe the molecular interaction between an encaged gas molecule and an H_2O molecule from the cavity wall, which is directly related to lowering the chemical potential of H_2O in the clathrate phase according to equations (2)–(4). In the context of determination of interatomic forces of gases, Lennard-Jones & Devonshire (1937) were astonished by the power of the equation of state from van der Waals (1873) but noticed its failure for dense gases. They introduced a cell theory by means of statistical mechanics for gas molecules whose average position is something like an atom in a liquid or a crystal. Platteeuw & van der Waals (1958) applied this theory to describe molecular

Table 4. *Henry's constants for equation (14) and partial molar volume of gases at infinite dilution in H_2O used in equation (15)*

Gas	a_0	a_1	a_2	a_3	a_4	v^{∞}_{gas} ($cm^3 mol^{-1}$)
CO_2 (Ref. 1)	−6.8346	1.2817×10^4	-3.7668×10^6	2.997×10^8	–	$58.9 - 0.08 \times T$*
CH_4 (Ref. 2)	9.881539	9864.392	-2.150256×10^6	8.810241×10^7	–	$\exp(3.205 + 0.00123 \times T)$
N_2 (Ref. 3)	−4.857	1.87007×10^4	9.674615×10^5	–	–	35.7†
C_2H_6 (Ref. 2)	−205.6101	2.624901×10^5	-1.128303×10^8	2.159875×10^{10}	-1.569604×10^{12}	$\exp(3.5808 + 0.00122 \times T)$

References: 1. Carroll *et al.* (1991); 2. Rettich *et al.* (1981); 3. Benson & Kraus (1976).
* From Bakker *et al.* (1996).
† From Moore *et al.* (1982).

forces in clathrate cavities, using the Lennard-Jones 12–6 potential function (Jones 1924). McKoy & Sinanoglu (1963) compared several molecular potential function and they concluded that the Kihara potential (Kihara 1953) predicts better dissociation pressures for gas hydrates of rod-like molecules, such as CO_2, N_2, and C_2H_6. Unlike the Lennard-Jones 12–6 potential, the Kihara potential takes into account the shape and the size of encaged molecules. Unfortunately, the Kihara potential is not the best potential function to describe the properties of H_2O molecules, the indispensable counterpart of molecular interaction in clathrates. However, this potential is eminately useful for gases like CO_2, CH_4, N_2 and C_2H_6. The spherical form of the Kihara potential (Tee *et al.* 1966) was used solely in later studies of clathrate modelling:

$$\Gamma(r) = 4\varepsilon_{ij}\left\{\left(\frac{\sigma_{ij}-2a_{ij}}{r-2a_{ij}}\right)^{12}-\left(\frac{\sigma_{ij}-2a_{ij}}{r-2a_{ij}}\right)^{6}\right\} \tag{16}$$

where Γ is intermolecular potential as a function of the distance (r) between molecules i and j, ε is the minimum potential energy, σ is the distance between two molecules for zero potential energy and a is the radius of impenetrable molecule cores. Bakker *et al.* (1996) noted the necessity for clarification of the application of the Kihara potential functions in clathrate modelling because many different notation methods for equal formulae have been used in the literature (e.g. Kihara 1953; McKoy & Sinanoglu 1963; Tee *et al.* 1966; Parrish & Prausnitz 1972; Avlonitis 1994). The transparency of clathrate stability modelling was seriously mystified by this variation. The parameters in equation (16) are all defined from the centre of molecules, which is a direct and clear method to describe potentials and which avoids any double standards.

The interaction parameters between unalike molecules, i.e. gas and H_2O, were originally obtained from classical mixing rules:

$$\varepsilon_{ij} = \sqrt{\varepsilon_i \varepsilon_j}$$
$$\sigma_{ij} = \frac{\sigma_i + \sigma_j}{2} \qquad (i \neq j). \tag{17}$$
$$a_{ij} = \frac{a_i + a_j}{2}$$

The Kihara parameter values for H_2O (Table 5) were originally based on theoretical considerations and indirect obtained values from argon gas hydrate (van der Waals & Platteeuw 1959). The core radius for a H_2O molecule is assumed to be 0 (McKoy & Sinanoglu 1963), which reduces the potential function to a Lennard-Jones 12–6 function. Holder *et al.* (1980) and John *et al.* (1985) obtained empirical values for ε and σ for H_2O molecules from experimental data on CH_4 gas hydrates (Table 5) using the values for pure CH_4 and the mixing rules from equation (17). These values are markedly different to the theoretical values from van der Waals & Platteeuw (1959), which illustrates the diversity of describing the molecular potential of H_2O molecules. The Kihara parameters for CO_2, CH_4, N_2, and C_2H_6 molecules (Table 5) are obtained directly both from second virial coefficient and from viscosity data from Tee *et al.* (1966). They give several sets of values for these parameters based on different independent data sets, and they give smoothed values from unified correlations, which are favoured in most clathrate modelling literature (e.g. Avlonitis 1994). However, unsmoothed parameters which are based on a larger data set, and which are also obtained from independent sources, are preferred in this study.

Table 5. *Kihara parameters for similar molecule interactions*

Gas	ε/k (K)	σ (pm)	a (pm)
H_2O (Ref. 1)	167.0	249.45	0
(Ref. 2)	115.5	375.1	0
(Ref. 3)	102.134	356.438	0
CO_2 (Ref. 4)	469.73	350.1	68.05
CH_4 (Ref. 4)	232.20	350.5	38.34
N_2 (Ref. 4)	97.31	366.1	0
C_2H_6 (Ref. 4)	425.32	397.7	56.51

References: 1. van der Waals & Platteeuw (1959); 2. Holder *et al.* (1980); 3. John *et al.* (1985); 4. Tee *et al.* (1966).

The molecular potential $w(r)$ in spherically symmetrical cells in clathrate structures, which McKoy & Sinanoglu (1963) designed for the Kihara potential was modified by Bakker *et al.* (1996) to do justice to equation (16):

$$w(r) = 2Z\varepsilon_{ij}\left\{\frac{(\sigma_{ij}-2a_{ij})^{12}}{rR^{11}}\left(\delta^{10}+\frac{2a_{ij}}{R}\delta^{11}\right)-\frac{(\sigma_{ij}-2a_{ij})^{6}}{rR^{5}}\left(\delta^{4}+\frac{2a_{ij}}{R}\delta^{5}\right)\right\} \tag{18a}$$

$$\delta^n = \frac{1}{n}\left\{\left(1-\frac{r}{R}-\frac{2a_{ij}}{R}\right)^{-n}-\left(1+\frac{r}{R}-\frac{2a_{ij}}{R}\right)^{-n}\right\} \tag{18b}$$

Table 6. *Coordination number* Z *and approximate radius* R *of small and large spherical cavities in clathrate Structure I and II*

	Structure I		Structure II	
	Small cavity (Pentagonal dodecahedron)	Large cavity (Tetrakaidecahedron)	Small cavity (Pentagonal dodecahedron)	Large cavity (Hexakaidecahedron)
Z	20	24	20	28
R (pm)*	387.5	430.0	387.0	470.3

* From John & Holder (1981).

where r is the distance from the centre of the cavity, Z and R are the coordination number and the cell radius of a type of cavity (Table 6), respectively, n is either 4, 5, 10 or 11. The cell radii are obtained from John & Holder (1981) who extensively studied deviations from the cavity symmetry according to van der Waals & Platteeuw (1959). The coordination number Z is set equal to the vertices of the cavities, unlike the estimation of effective coordination numbers by John & Holder (1981). John & Holder (1981) and John *et al.* (1985) noted that the binary interaction parameters in equations (16) and (18) calculated with the arbitrary mixing rules from equation (17) do not result in an accurate reproduction of clathrate stability conditions. They incorporate second neighbour molecular interactions and the asymmetry of such interactions, modifying postulate (e) from van der Waals & Platteeuw (1959).

A different approach to clathrate modelling is chosen in this study. The Kihara parameters of binary gas–H_2O interactions in clathrate cavities can be directly obtained from minimizing differences between model predictions and experimental data on clathrate melting conditions. This method was introduced by Saito *et al.* (1964) for CH_4, N_2 and argon gas hydrates. Subsequently, they used the previously mentioned mixing rules (equation (17)) and the theoretical values for a H_2O molecule to estimate the molecular potential parameters for pure gases according to the Lennard-Jones 12–6 potential. This method has been adopted by, for example, Parrish & Prausnitz (1972), Anderson & Prausnitz (1986), Dubessy *et al.* (1992) and Bakker *et al.* (1996) for the Kihara potential function. A very important implication of this method is that all irregularities and deviations in principle assumptions for other parameters are projected onto these Kihara parameters. The first step of this method avoids uncertainties in the arbitrarily defined mixing rules and in the molecular potential function for pure H_2O in the clathrate phase. Prausnitz *et al.* (1986) give a general overview of many variations on arbitrarily mixing rules like equation (17), which reinforces its preferred omission in this study. Consequently, this study has two significant uncertain steps less than models which include equation (17) to calculate gas–H_2O interactions in clathrate phases (e.g. John *et al.* 1985; Avlonitis 1994). In this study, only the core radius for unalike molecule interaction is obtained from the geometrical mean (equation (17)) of values given in Table 5 for pure components.

Optimum Kihara parameters in the clathrate phase

Unsmoothed experimental data on clathrate phase equilibria for pure CO_2, CH_4, N_2, and C_2H_6 gas hydrates (Table 7) are used to determine optimum Kihara parameters ε and σ between an encaged gas molecule and a cage-forming water molecule. The large amount of available data allows a careful discrimination of those data which appear to be inconsistent with the system. For example, data on C_2H_6 gas hydrate from Roberts *et al.* (1940) are not used in this study because they are not consistent with other data sets in the same range of clathrate melting temperatures. Data on clathrate melting above 210 MPa are also excluded in this study, because many other parameters, like gas solubility and fugacity, that play an important role in clathrate modelling cannot be accurately calculated at higher pressures. For example, experimental data on CH_4 and N_2 gas hydrates above 210 MPa from Marshall *et al.* (1964) are excluded for this reason.

Optimum Kihara parameters are found after a lengthy search within ε/k–σ diagrams (Fig. 4 and Table 8). These parameters are systematically varied, and for each set of ε/k–σ values the average deviation between the model and all experimental data has been calculated. The

Table 7. *Available experimental data*

Gas hydrate	Literature	Amount of data
CO_2	Deaton & Frost (1946)	19
	Unruh & Katz (1949)	5
	Larson (1955)	38
	Takenouchi & Kennedy (1965)	15
	Robinson & Metha (1971)	7
	Ng & Robinson (1985)	9
	Adisasmito *et al.* (1991)	9
	Dholabhai *et al.* (1993)	4
	Englezos & Hall (1994)	6
CH_4	Deaton & Frost (1946)	13
	Kobayashi & Katz (1949)	4
	McLeod & Campbell (1961)	10
	Marshall *et al.* (1964)	20
	Jhaveri & Robinson (1965)	8
	Galloway *et al.* (1970)	4
	Verma *et al.* (1975)	7
	De Roo *et al.* (1983)	9
	Adisasmito *et al.* (1991)	11
	Dickens & Quinby–Hunt (1994)	7
N_2	van Cleeff & Diepen (1960)	39
	Marshall *et al.* (1964)	14
	Jhaveri & Robinson (1965)	8
C_2H_6	Roberts *et al.* (1940)	20
	Deaton & Frost (1946)	20
	Reamer *et al.* (1952)	4
	Galloway *et al.* (1970)	3
	Holder & Grigoriou (1980)	7
	Holder & Hand (1982)	7
	Ng & Robinson (1985)	8
	Avlonitis (1988)	10
	Englezos & Bishnoi (1991)	6

numerical approach of this method takes into account the chemical potential of both clathrate structures, I and II. Obviously, the most stable configuration has the lowest chemical potential. The boundary between clathrate Structure I and II is defined by certain σ value and it is independent upon ε/k values (Fig. 4). Clathrate Structure II appears to be stable at lower σ values than Structure I for CO_2, CH_4 and N_2 gas hydrates. This phase change is also temperature dependent, therefore only the boundary near Q_1 conditions is illustrated in Fig. 4. The boundary moves only several pm to lower σ values at higher temperatures. These estimations imply that a clathrate structure with larger cavities is more stable if encaged gas molecules can get closer to the wall of the cavities. C_2H_6 gas hydrate has a clathrate Structure I over the entire range of σ and ε/k values illustrated in Fig. 4d. Contours of equal deviation have been draw in these diagrams (Fig. 4). The very irregular shape of the 5% deviation contour indicates the complexity of a systematic approach. The pattern in Fig. 4 is an interference between best-fits in both clathrate structures, which is clearly demonstrated by the discontinuity at the phase boundary. Minima in average deviation are present in both parts of the diagrams. The intention of the method is to choose the lowest minimum as a solution for optimum Kihara parameters. The position of minima for CO_2, N_2 and C_2H_6 (Table 8) are consistent with their observed clathrate structures, however, that for CH_4 appears to be in the Structure II field, close to the phase boundary. These thermodynamic considerations imply that CH_4 has a clathrate Structure II at Q_1 conditions, and changes to clathrate Structure I above 292 K. However, it is well known that relatively small CH_4 molecules form a clathrate Structure I, which has been measured from X-ray diffraction data by von Stackelberg & Müller (1954). Consequently, the minimum in the clathrate Structure I field has to be chosen for CH_4 gas hydrate (Table 8), which does not differ very much in magnitude from the lowest minimum. Small differences in chemical potential between clathrate Structure I and Structure II may allow the formation of the metastable phase due to small growth irregularities, or the presence of impurities. The diagram for N_2 gas hydrates has a similar pattern with three minima (Fig. 4c), but the middle minimum in the clathrate Structure II field has a significant lower average deviation than the other minima. The interpretation of these thermodynamic calculations are consistent with the findings of Davidson *et al.* (1987) who were the first to identify a clathrate Structure II for N_2 gas hydrate from powder diffraction patterns. C_2H_6 gas hydrate has the least pronounced minimum, which is directly related to the relatively small amount of experimental data used for the optimization.

The low average deviation for all types of pure gas hydrates (Fig. 4 and Table 8) illustrates the excellent fit between this clathrate model and the experimental data. The error values illustrated in Fig. 4 are average values, which may differ from error values for individual data points. Therefore, the deviation of each individual experimental data point is given in Fig. 5. Most individual data are located within 2% accuracy for CO_2 (Fig. 5a), 4% for CH_4 (Fig. 5b), 2% for N_2 (Fig. 5c) and 4% for C_2H_6 (Fig. 5d) from model predictions. This accuracy is improved even further if the error in measurements of individual datum is taken into account.

The results of these optimalization are strongly dependent on other parameters used in this clathrate stability model. A thorough error

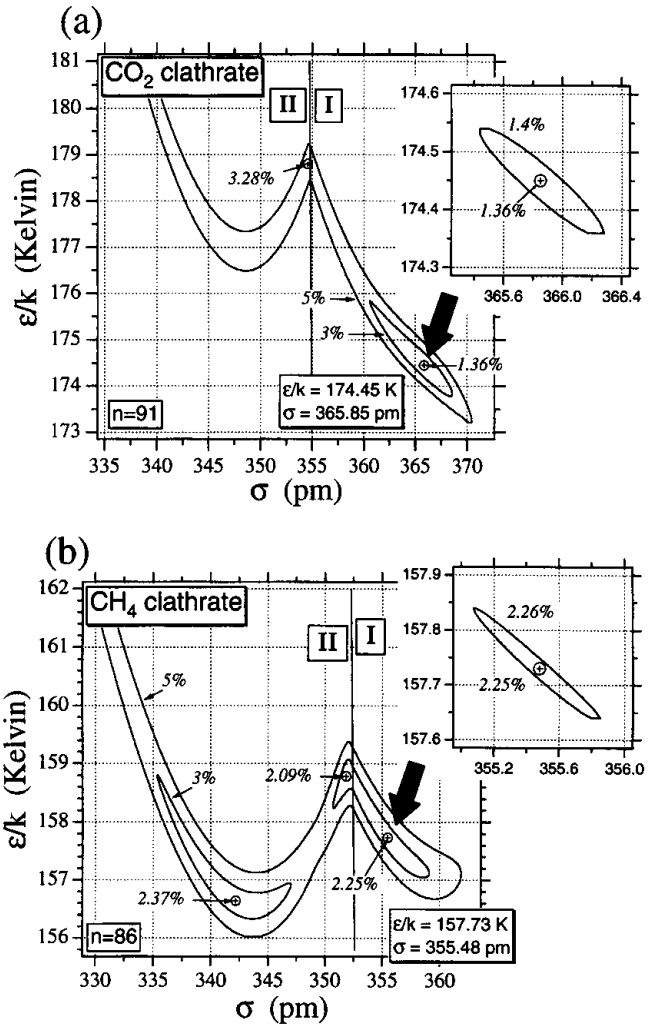

Fig. 4. $\sigma-\varepsilon/k$ diagrams for (**a**) CO_2, (**b**) CH_4, (**c**) N_2, and (**d**) C_2H_6 with contours of equal average deviation between the clathrate stability model and experimental data. I is clathrate Structure I; II is clathrate Structure II; n is the amount of used experimental data.

analysis by Bakker *et al.* (1996) illustrates that mainly uncertainties in the Kihara core parameter a and chemical potential of the empty clathrate phase at standard conditions $\mu_{H_2O}^{empty}(ref)$ influence the position of the best solution for the two other Kihara parameters ε and σ. The main variation is obtained in ε/k values (Bakker *et al.* 1996, p. 1667, Fig. 12). An error indication of approximately 2 pm is obtained for σ values, and approximately 4 K for ε/k values. This error indications are only slightly improved if more data are available.

Best-fit estimations of clathrate melting conditions in the presence of a liquid-like gas-rich phase for clathrates with a Q_2 point (see Fig. 1), like CO_2 and C_2H_6, are separated from those in the presence of a vapour-like gas-rich phase, below Q_2 conditions. Deviations between calculated clathrate melting pressures and observed pressures at selected temperatures are, in general, very large above Q_2 conditions due to the relatively steep slope of the melting curve. This apparently bad fit is an artefact, and the inverse method, i.e. comparison of clathrate melting temperatures at selected pressures, gives much better results at these conditions.

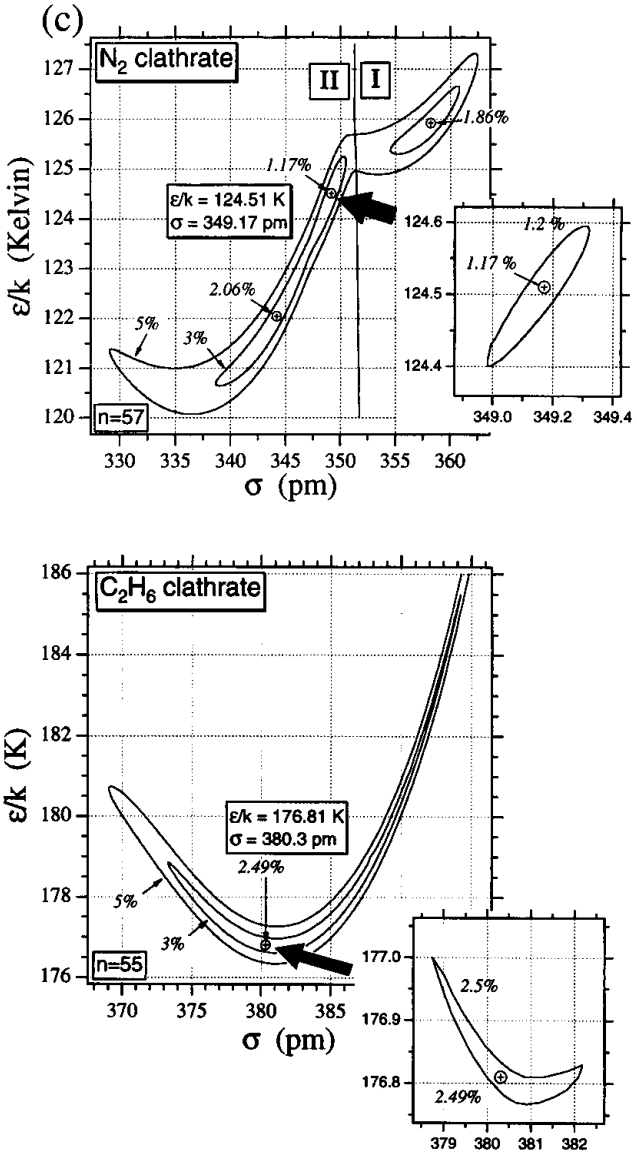

Fig. 4. (*cont.*)

Unfortunately, experimental data above Q_2 conditions are highly inconsistent for CO_2 gas hydrates (Takenouchi & Kennedy 1965; Ng & Robinson 1985) and C_2H_6 gas hydrates (Roberts *et al.* 1940; Ng & Robinson 1985). Using the optimum Kihara parameters obtained from below Q_2 conditions for CO_2 gas hydrate results in overestimated pressures at selected temperatures above Q_2 conditions. For CO_2, the best solution is obtained from $\sigma = 364.74$ pm (Table 8), while ε/k remains unchanged. Differences between modelled and measured clathrate melting pressures at selected temperatures above Q_2 conditions may exceed 30% (Fig. 6a). The fit of

Table 8. *Best-fit solutions for Kihara parameters ε/k and σ for gas–H_2O molecular interactions in clathrate structures,* n *is the amount of experimental data used in the fitting procedure*

Gas hydrate	ε/k (K)	σ (pm)	n	Average deviation
CO_2	174.45	365.85	91	1.36%
		364.74*	19	–
CH_4	157.73	355.48	86	2.25%
N_2	124.51	349.17	57	1.17%
C_2H_6	176.81	380.3	55	2.49%

* Above Q_2 conditions.

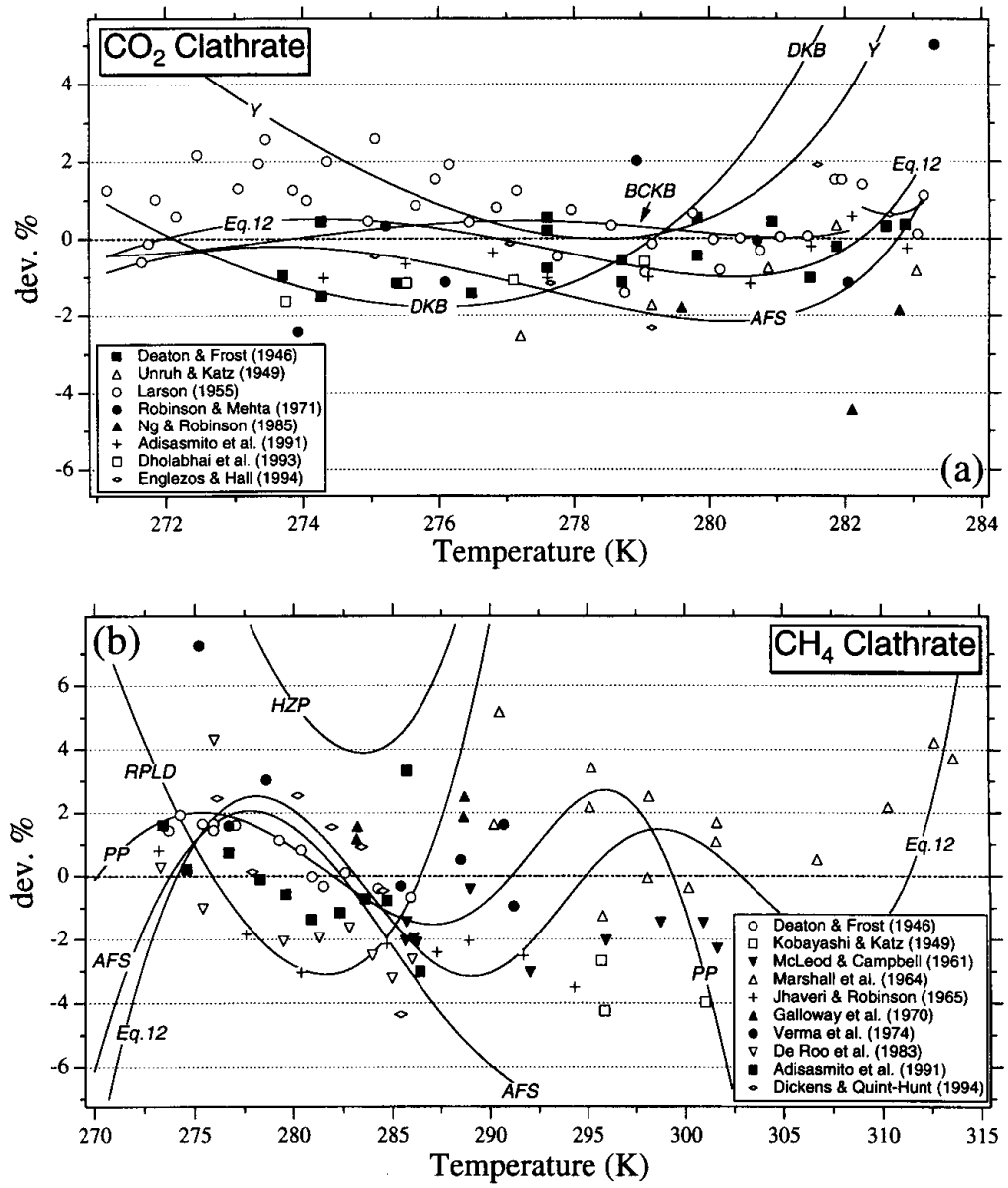

Fig. 5. Deviation of individual experimental data on clathrate stability conditions from (**a**) CO_2, (**b**) CH_4, (**c**) N_2, and (**d**) C_2H_6 gas hydrates to model predictions according to the estimated optimum Kihara parameters σ and ε/k in Fig. 4. Solid lines are comparisons for available purely empirical equations for clathrate-stability conditions: BCKB, Bozzo *et al.* (1975); HZP, Holder *et al.* (1988); AFS, Adisasmito *et al.* (1991); Y, Yerokin (1993); PP, Parrish & Prausnitz (1975); RPLD, De Roo *et al.* (1983); Eq. 12, equation (12) from this study.

the model to experimental data is improved at higher temperatures. The model produces the midpoint between experimental data sets, which makes it an acceptable mediator. The experimental data for C_2H_6 gas hydrate above Q_2 conditions are adequately reproduced by the σ value obtained at lower pressures (Fig. 6b), although the scatter in data from Roberts *et al.* (1940) do not allow any conclusive interpretation.

The quadruple points for each pure gas

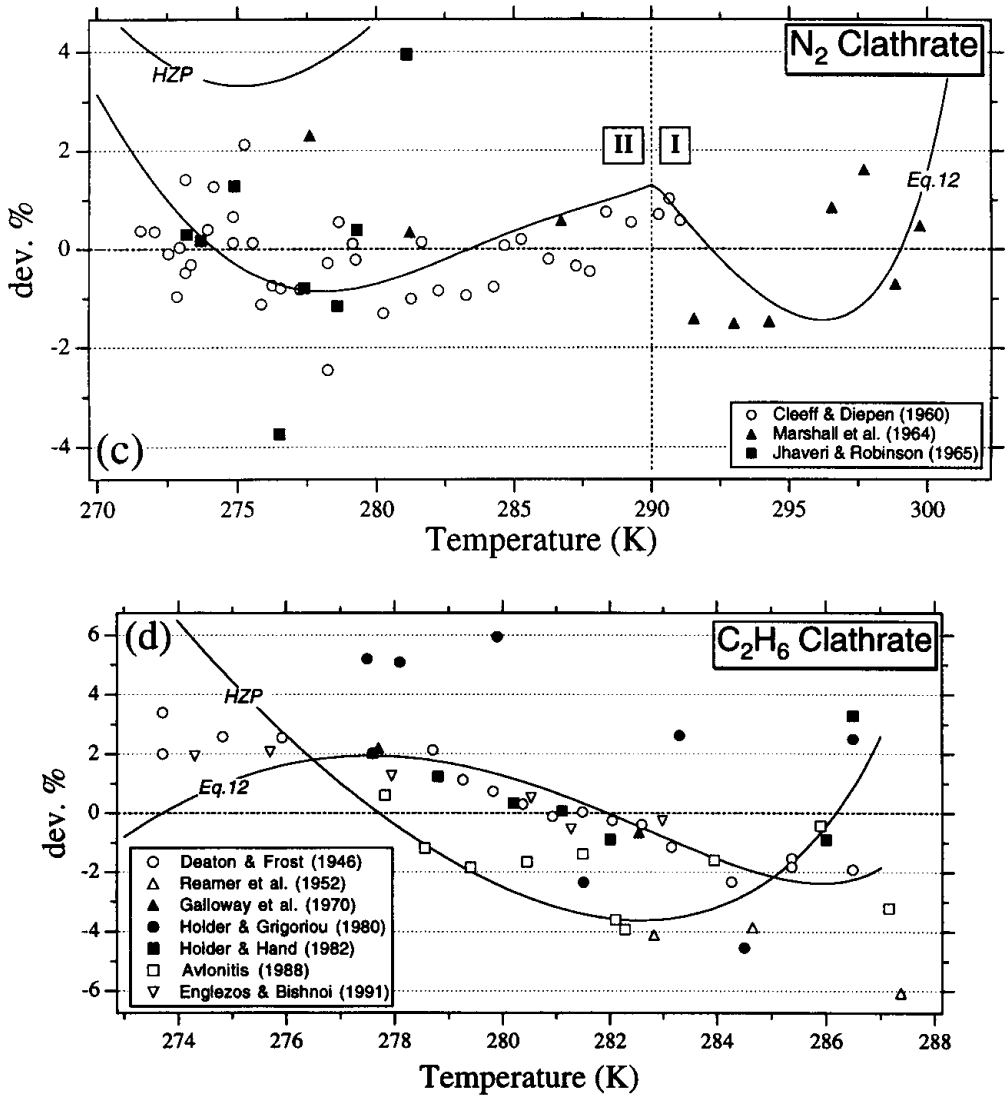

Fig. 5. (*cont.*)

hydrate have been calculated from these optimum Kihara parameters (Table 9). Q_2 points are obtained from the intersection of the clathrate melting curve and saturation curve for pure gases. Q_1 points are calculated from the intersection of clathrate melting curves in equilibrium with ice and liquid.

Comparison to literature

Bakker *et al.* (1996) already illustrated large differences for Kihara parameters for CO_2–H_2O molecular interactions in clathrate structures. At first sight, reported Kihara parameters for gas–water interactions are astonishingly different in the literature (Table 10). To eliminate the effect of the core radius a, molecule interactions are compared from the edge of the impenetrable core as a reference distance ($\sigma - 2a$). The pioneering study from McKoy & Sinanoglu (1963) show large deviations from this work, in particular ε/k values are extremely overestimated in their study. The second large anomaly is the study from John *et al.* (1985), whose ε/k value for CO_2 gas hydrate differs

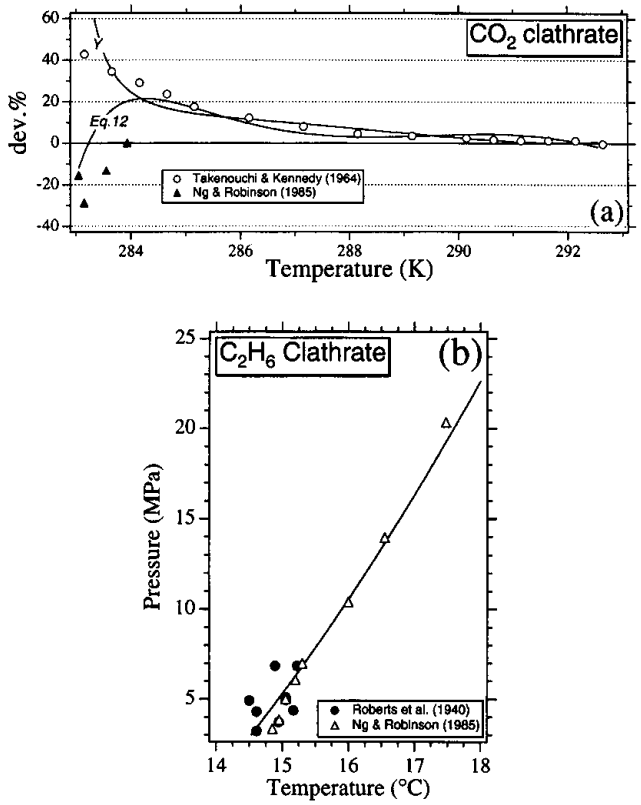

Fig. 6. (**a**) Deviation of individual experimental data from CO_2 gas hydrate at high pressures, above Q_2 conditions. Solid lines are comparisons with purely empirical equations from Yerokin (Y) and this study (Eq. 12). (**b**) T–P diagram with a modelled clathrate stability curve for C_2H_6 gas hydrate (solid line) and experimental data from Roberts *et al.* (1940) and Ng & Robinson (1985), above Q_2 conditions.

by up to 30% from this study. This variation is expected because John *et al.* (1985) used a different approach to clathrate modelling and included second neighbour interactions, as previously described. For the other studies, the relative deviation in $\sigma - 2a$ and ε/k values are, in general, less 10%, which still greatly exceeds the absolute error range estimated in this study. This variation corresponds perfectly to the amount of experimental data used to fit these parameters. The scatter of experimental data in Fig. 5 indicates a maximum difference of *c.* 12%, which is similar to the variation found for Kihara parameters in several studies (Table 10). Thus, the ambiguous disagreement, which has been recognized in the literature (e.g. Sloan 1990; Avlonitis 1994), is merely a reflection of the use of an insufficient amount of data. This interpretation justifies the necessity to use the most accurate values for gas solubilities, fugacities and thermodynamic constants, in addition to a large amount of independently obtained experimental data, as demonstrated in this study.

Differences in optimum Kihara parameters for N_2 gas hydrates may result from its only recently discovered clathrate Structure II (Davidson *et al.* 1987), which is in contradiction to the classical size–structure rule of von Stackelberg & Müller (1954). Only Lundgraad & Mollerup (1991) and Avlonitis (1994) modelled the N_2 according to Structure II clathrates. For example, Parrish & Prausnitz (1972), Anderson & Prausnitz (1986) and Dubessy *et al.* (1992) modelled N_2 according to Structure I clathrates, which obviously must result in different values for the optimized Kihara parameters.

Several purely empirical equations are compared to model predictions and experimental data in Figs 5 and 6. Most empirical equations for pure CO_2 gas hydrate are accurately repro-

Table 9. *Quadruple points Q_1 and Q_2 for pure CO_2, CH_4, N_2, and C_2H_6 gas hydrates*

Gas hydrate	Q_1		Q_2	
	T (K)	P (MPa)	T (K)	P (MPa)
CO_2	271.66	1.041	282.961	4.481
CH_4	272.85	2.583	–	–
N_2	271.85	14.253	–	–
C_2H_6	273.13	0.483	287.798	3.348

ducing experimental data. The equation from Bozzo *et al.* (1975) is very similar to our model predictions, and, therefore, is most accurately producing clathrate stability conditions between Q_1 and Q_2. The equation from Dholabhai *et al.* (1993) and Yerokhin (1993) increasingly deviate from both this model and the experimental data at temperatures above 280 K and near Q_1 conditions. Above Q_2 conditions (Fig. 6a) the equation from Yerokhin (1993) accurately reproduces the data from Takenouchi & Kennedy (1965). The empirical equations for pure CH_4 gas hydrates are, in general, less accurate. The equation according to Parrish & Prausnitz

Table 10. *Comparison of Kihara parameters $\sigma - 2a$ and ε/k for gas–H_2O interactions*

Gas hydrate	Literature	ε/k (K)	Deviation (%)	$\sigma - 2a$ (pm)	Deviation (%)
CO_2	MS	309	77	299.3	0.5
	PP	169.09	−3.1	296.81	−0.3
	JPH	227.39	30	280.869	−5.7
	AP	169.44	−2.9	295.61	−0.7
	LM	162.37	−6.9	335.43	12.6
	DTC	170.0	−2.6	295.8	−0.7
	A	172.0	−1.4	290.4	−2.5
	This study	174.45		297.8	
CH_4	MS	205	30	298.5	−5.9
	PP	153.17	−2.9	323.98	2.2
	HCP	148.88	−5.6	343.45	8.3
	JPH	141.987	−10	327.269	3.2
	AP	153.39	−2.8	325.78	2.7
	LM	151.41	−4.0	326.6	3.0
	DTC	152.0	−3.6	327.0	3.1
	A	153.8	−2.5	325	2.5
	This study	157.73		317.16	
N_2	MS	124	−0.4	309.0	−11.5
	PP	127.95	2.8	361.42	3.5
	JPH	127.422	2.3	316.319	−9.4
	AP	128.57	3.3	326.77	−6.4
	LM	125.94	1.1	331.16	−5.2
	DTC	126.25	1.4	328.0	−6.1
	A	127.0	2.0	318.3	−8.8
	This study	124.51		349.17	
C_2H_6	MS	609	244	230.7	−29
	PP	174.97	−1.0	331.80	2.4
	JPH	200.397	13.4	322.619	−0.4
	AP	175.94	−0.5	343.81	6.1
	LM	176.89	0.1	347.32	7.2
	DTC	175.0	−1.0	344.0	6.2
	A	184.1	4.1	343.0	5.9
	This study	176.79		323.99	

MS, McKoy & Sinanoglu (1963); PP, Parrish & Prausnitz (1972); HCP, Holder *et al.* (1980); JPH, John *et al.* (1985); AP, Anderson & Prausnitz (1986); LM, Lundgaard & Mollerup (1991); DTC, Dubessy *et al.* (1992); A, Avlonitis (1994).

(1972) is in good agreement with our model predictions and remains within 3% accuracy from Q_1 up to 300 K. The equations from De Roo *et al.* (1983) and Adisasmito *et al.* (1991) are only applicable up to 288 K. Near Q_1 conditions none of these equations are able to reproduce the experimental data. The equation according to Holder *et al.* (1988) is unable to reproduce any experimental data at all, and extensively overestimates the model predictions. Equation (12) from this study is the sole empirical equation which can be used up to 313 K for CH_4 gas hydrate (Fig. 5b). For N_2 gas hydrates (Fig. 5c) the equation from Holder *et al.* (1988) is, again, not related to any experimental data and unable to reproduce model predictions. Equation (12) from this study accurately reproduces experimental data between Q_1 and 300 K, and is in close agreement with the model. Both equation (12) and the equation from Holder *et al.* (1988) accurately reproduce experimental data of C_2H_6 gas hydrate (Fig. 5d). Although, purely empirical equations can be easily applied by solving a simple mathematical equation, these comparisons illustrate its limited use. In fact, most of them can only be used for pure gas hydrates and in limited ranges of clathrate stability conditions.

Clathrate equilibria of binary guest mixtures

It has been demonstrated that the previously described model very accurately reproduces clathrate stability conditions for pure gas hydrates over a wide range of temperatures, including all available experimental data. The definitions for this clathrate stability model (equations (2)–(4)) allow application to calculate any type of gas mixture in equilibrium with clathrate. Therefore, experimental data of binary guest mixtures are compared to the model prediction. An unexpected large difference between the calculated and modelled clathrate melting pressure at selected temperatures is observed, which greatly exceeds those predictions for pure gas hydrates. This result is similar to prediction from other classical clathrate stability models, which are unable to accurately reproduce mixed gas hydrate stability conditions.

A method has been developed in this study to describe this discrepancy systematically. Available data on gas mixture composition of the vapour phase and melting temperature and pressure of the clathrate phase (Table 11) allow calculation of the amount of energy that is missing in the original equilibrium formula (equation (1)). This missing chemical potential

Table 11. *Experimental data for binary gas hydrates*

Binary gas hydrate	Literature	Amount of data
CO_2–CH_4	Unruh & Katz (1949)	17
	Adisasmito *et al.* (1991)	42
CH_4–N_2	Jhaveri & Robinson (1965)	63
CH_4–C_2H_6	Deaton & Frost (1946)	24
	McLeod & Campbell (1961)	16
	Holder & Grigoriou (1980)	15

is attributed to the clathrate and is suggested to be an excess Gibbs free energy function (equation (19)) which depends on the gas mixture composition and temperature

$$\mu_{H_2O}^{clath} = \mu_{H_2O}^{empty} + RT\sum_i v_i \ln\left(1 - \sum_M y_{Mi}\right) + G^{excess}(x, T). \quad (19)$$

Physically, the G^{excess} function is suggested to result from non-ideal interactions between cavities which are occupied by different types of guest molecules. Thompson (1967) introduced the Margules equations (Margules 1895) to characterize non-ideality for binary crystalline solution in petrological and geochemical research. The Margules model describes an excess thermodynamic function as a power series expressed in mole fractions of the components involved. Thompson (1967) used symmetrical (equation (20a)) and asymmetrical (equation (20b)) excess functions to obtain the position of solvi for immiscible mineral solutions. He noted that most real solutions are asymmetric to some degree:

$$G^{excess} = X_1 X_2 W_G \quad (20a)$$

$$G^{excess} = X_1 X_2 (W_{G1} X_2 + W_{G2} X_1) \quad (20b)$$

where W_G are interchange energies which depend only on temperature, not on composition. In this study the strong asymmetry for clathrate phases needs a modification of equation (20) to be able to characterize clathrate excess functions:

$$G^{excess} = X_1 X_2 (W_{G1} X_2^2 + W_{G2} X_1^2). \quad (21)$$

The temperature dependence of W_G is described according to a second-order polynome:

$$W_G = w_0 + w_1 T_C + w_2 T_C^2 \quad (22)$$

where T_C is temperature in °C, and w_0, w_1 and w_2 are constant values for selected binary gas hydrates (Table 12). The derivation of these functions from experimental data is illustrated in detail in the next paragraph using CO_2–CH_4

Table 12. *Constants for the modified Margules formulae in equation (22)*

Mixed gas hydrate		w_0	w_1	w_2
CO_2–CH_4	$W_G^{CO_2}$	119.43	16.792	–
	$W_G^{CH_4}$	33.699	7.5437	–
CH_4–N_2	$W_G^{CH_4}$	140.45	−128.58	5.9032
	$W_G^{N_2}$	286.32	−34.053	0.42591
CH_4–C_2H_6	$W_G^{CH_4}$	2057.7	−43.155	−1.7486
	$W_G^{C_2H_6}$	−1756.6	86.956	−0.70654

mixed gas hydrate as an example. The summation over all binary excess functions can be used in ternary and higher-order guest mixture gas hydrates.

Several complications are linked to the application of the excess functions (equations (21) and (22)). First, the composition of gas hydrates is difficult to obtain by direct chemical analysis (e.g. Dharmawardhama *et al.* 1980). Hydrate composition is subject to large experimental uncertainties. Parrish & Prausnitz (1972) mentioned that only the vapour phase composition, which is in equilibrium with the clathrate phase, is important in process design application. In this study, the filling of the clathrate structures is theoretically obtained with the sophisticated treatment from van der Waals & Platteeuw (1959). To avoid any systematic errors in modelling and large experimental uncertainties, it is preferable to compare the calculated excess function for the clathrate phase to the mole fraction in the vapour phase. Distribution coefficients between both phases must be used in order to obtain true excess functions for the clathrate phase. Second, in the previous section two values are given for the optimized Kihara parameter σ for pure CO_2 gas hydrate (Table 8), which were obtained from equilibria with a CO_2-rich gas phase at high densities (above Q_2 conditions) and low densities (below Q_2 conditions). Clathrate melting in equilibrium with a CO_2-rich fluid phase with intermediate densities, between 51 and 332 cm^3/mol^{-1}, do not occur, which is a direct consequence of the intersection with the saturation curve for pure CO_2. Addition of small amounts of CH_4 or N_2 reduces the liquid–vapour equilibria of the fluid phase to lower temperatures (see Fig. 1), and subsequently, these intermediate densities do occur in mixed gas hydrates stability calculations. Therefore, a transition zone has to be defined for the σ parameter from CO_2–H_2O interactions to describe its alteration as a function of molar volume of the gas-rich phase:

$$\sigma_{CO_2} = X_V \times \sigma_{liq} + (1 - X_V) \times \sigma_{vap} \quad (23a)$$

$$X_V = \frac{(332 - V_M)}{(332 - 51)} \quad (23b)$$

where V_M is the molar volume of the gas-rich phase, X_V varies between 0 and 1. X_V is 1 for molar volumes lower than 51 $cm^3\,mol^{-1}$ (high densities), and 0 for molar volumes higher than 332 $cm^3\,mol^{-1}$ (low densities). An important implication of the use of excess functions is the possibility of the demixing of mixed gas hydrates into pure gas hydrates at lower temperatures. Although this has not yet been described in the literature, it is proposed as a possible process in natural gas hydrates.

CO_2–CH_4 gas hydrate

CO_2–CH_4 gas hydrate forms a Structure I clathrate over the entire compositional range, which is obviously inherited from the pure end-member CO_2 and CH_4 gas hydrates. The equation of state according to Duan *et al.* (1992*a*, *b*) is selected to calculate the fugacities of the components in CO_2–CH_4 mixtures with small amounts of H_2O. This equation of state was previously selected for both pure CO_2 gas hydrate and pure CH_4 gas hydrate.

Experimental data from Unruh & Katz (1949) and Adisasmito *et al.* (1991) are compared to model predictions as presented in the previous section, without an excess energy function. The difference between calculated and measured clathrate melting pressure at selected temperatures approaches 20% for mixtures containing 40 mol% CO_2, which greatly exceeds the accuracy of the pure end-members. The amount of missing energy is calculated for each individual data point (Table 13 and Fig. 7) in order to be able to perform a systematic analysis of these differences. Most data from Unruh & Katz (1949) are compatible with those from Adisasmito *et*

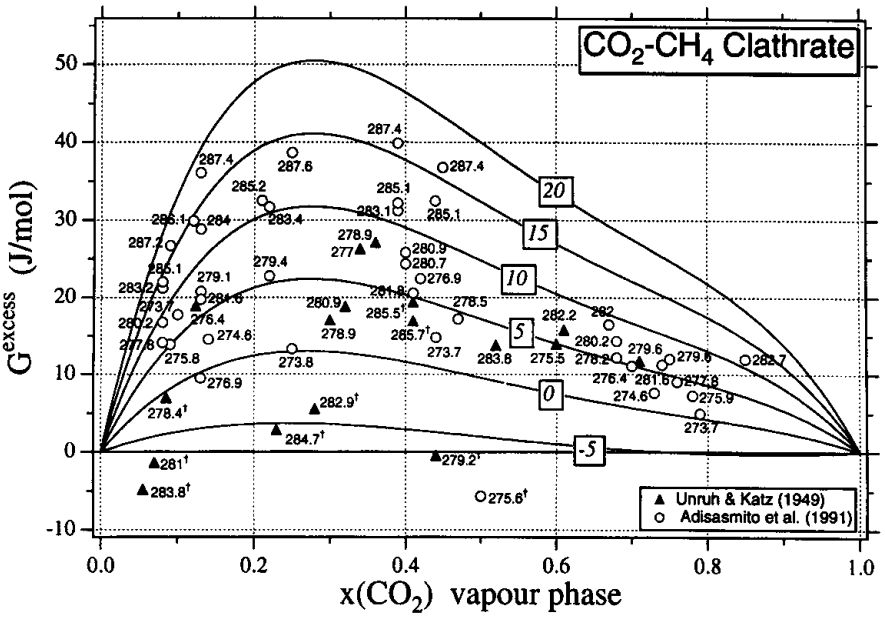

Fig. 7. $G^{excess}-X$ diagram for CO_2–CH_4 mixed gas hydrate. Numbered temperatures for individual data points are in Kelvin. Curved solid lines are modelled G^{excess} values according to equations (21) and (22) at selected temperatures (squared numbers in °C). Experimental data points marked with an † are excluded from the estimation of interchange energies W_G.

al. (1991), although their scatter is much larger. Figure 7 demonstrates an increase in excess energy at higher temperatures and intermediate compositions. First, a $G^{excess}-T$ diagram is constructed (Fig. 8a) with isopleths from the composition of the vapour phase. Data close to a selected isopleth are projected. This diagram clearly illustrates individual data points that are inconsistent with the general trend outlined by most data, and it allows a careful selection procedure. For example, calculated G^{excess} values of data from Unruh & Katz (1949) for the 0.42 isopleth (Fig. 8a) are too low, and, therefore, they are not included in a best-fit line estimation to describe the temperature dependency of G^{excess}. For the 0.73 isopleth (Fig. 8a), all data are consistent. The best-fit method smooths calculated data and allows interpolation at selected temperatures. Second, a $G^{excess}-X$ diagram is constructed with these smoothed values for several vapour compositions at selected temperatures (Fig. 8b). An equation in the form of equation (21) is fitted to this data set by constantly arbitrarily varying the values for interchange energies W_G, until an acceptable fit is obtained. Third, these interchange energies for selected temperatures are plotted in a W_G-T diagram (Fig. 8c) to estimate a polynomal fit for the temperature dependency of W_G in the form of equation 22. The interchange energies for both CO_2 and CH_4 appear to increase linearly with temperature (Table 12). The asymmetry of the calculated isotherms in Fig. 7 is strongly dragged towards CH_4-rich compositions. Analysis based solely on one data set may result in very dissimilar estimated excess functions.

The CO_2 gas hydrate has two quadruple points at two defined temperatures and pressures, where four different phases are in stable configuration (Q_1 and Q_2), whereas CH_4 gas hydrate has only a Q_1 point (Table 9). Addition of small amounts of CH_4 to a CO_2-rich vapour phase in equilibrium with the clathrate phase transforms its Q_2 point into a limited line in a *TP*-diagram (Fig. 9), according to the classical phase rule. This line is defined by the intersection of the immiscibility field of a CO_2-rich liquid phase and a CH_4-rich vapour phase (e.g. Thiéry *et al.* 1994; Bakker 1997) and the clathrate melting curve. This immiscibility will retreat to lower temperatures as the amount of CH_4 in the gas mixture increases, whereas the clathrate melting curve moves to a much lesser extent. For a gas mixture of about 79 mol% CO_2 and 21 mol%

Table 13. *Measured clathrate stability conditions and calculated* G^{excess} *and mole fractions in the clathrate phase for binary* CO_2–CH_4 *gas hydrate*

Literature	Measured values				Calculated values	
	xCO_2(vap)	T (K)	P (MPa)	G^{excess} (J mol^{-1})	xCO_2(cla)	xCH_4(cla)
Adisasmito *et al.* (1991)	0.10	273.7	2.52	17.73	0.032	0.108
	0.09	275.8	3.10	13.86	0.029	0.111
	0.08	277.8	3.83	14.09	0.026	0.115
	0.08	280.2	4.91	16.73	0.026	0.116
	0.08	283.2	6.80	21.16	0.025	0.117
	0.08	285.1	8.40	22.00	0.025	0.119
	0.09	287.2	10.76	26.67	0.027	0.117
	0.14	274.6	2.59	14.52	0.041	0.099
	0.13	276.9	3.24	9.53	0.038	0.102
	0.13	279.1	4.18	20.77	0.038	0.103
	0.13	281.6	5.38	19.73	0.038	0.105
	0.13	284.0	7.17	28.80	0.037	0.106
	0.12	286.1	9.24	29.89	0.034	0.110
	0.13	287.4	10.95	36.06	0.035	0.109
	0.25	273.8	2.12	13.31	0.061	0.077
	0.22	279.4	3.96	22.74	0.055	0.086
	0.22	283.4	6.23	31.65	0.053	0.089
	0.21	285.2	7.75	32.51	0.051	0.093
	0.25	287.6	10.44	38.66	0.054	0.090
	0.44	273.7	1.81	14.78	0.085	0.051
	0.42	276.9	2.63	22.41	0.083	0.056
	0.40	280.7	4.03	24.33	0.079	0.092
	0.39	283.1	5.43	31.21	0.076	0.065
	0.39	285.1	6.94	32.15	0.074	0.068
	0.39	287.4	9.78	39.87	0.070	0.074
	0.50	275.6	1.99	−5.67	0.091	0.045
	0.47	278.5	2.98	17.17	0.087	0.051
	0.40	280.9	4.14	25.77	0.079	0.062
	0.41	281.8	4.47	20.55	0.079	0.061
	0.44	285.1	9.84	32.49	0.079	0.063
	0.45	287.4	9.59	36.77	0.076	0.068
	0.73	274.6	1.66	7.64	0.111	0.023
	0.70	276.4	2.08	11.07	0.108	0.027
	0.68	278.2	2.58	12.20	0.107	0.030
	0.68	280.2	3.28	14.33	0.106	0.032
	0.67	282.0	4.12	16.47	0.104	0.035
	0.79	273.7	1.45	5.00	0.115	0.018
	0.78	275.9	1.88	7.27	0.115	0.020
	0.76	277.8	2.37	9.10	0.113	0.023
	0.75	279.6	2.97	12.01	0.112	0.025
	0.74	281.6	3.79	11.24	0.111	0.028
	0.85	282.7	4.37	11.96	0.120	0.018
Unruh & Katz (1949)	0.34	277.0	2.84	26.29	0.073	0.066
	0.30	278.9	3.46	17.05	0.067	0.073
	0.36	278.9	3.43	27.13	0.075	0.065
	0.32	280.9	4.24	18.81	0.069	0.072
	0.28	282.9	5.17	5.55	0.063	0.079
	0.23	284.7	6.47	2.81	0.055	0.088
	0.60	275.5	1.99	13.94	0.100	0.036
	0.44	279.2	3.08	−0.45	0.084	0.055
	0.123	276.4	3.20	18.88	0.037	0.104
	0.085	278.4	3.95	6.98	0.027	0.114
	0.07	281.0	5.10	−1.41	0.023	0.119
	0.055	283.8	6.89	−4.86	0.019	0.124
	0.71	279.6	3.00	11.75	0.109	0.029
	0.61	282.2	4.27	15.78	0.099	0.041
	0.52	283.8	5.27	13.77	0.089	0.052
	0.41	285.5	6.89	19.37	0.076	0.066
	0.41	285.7	7.00	16.93	0.076	0.066

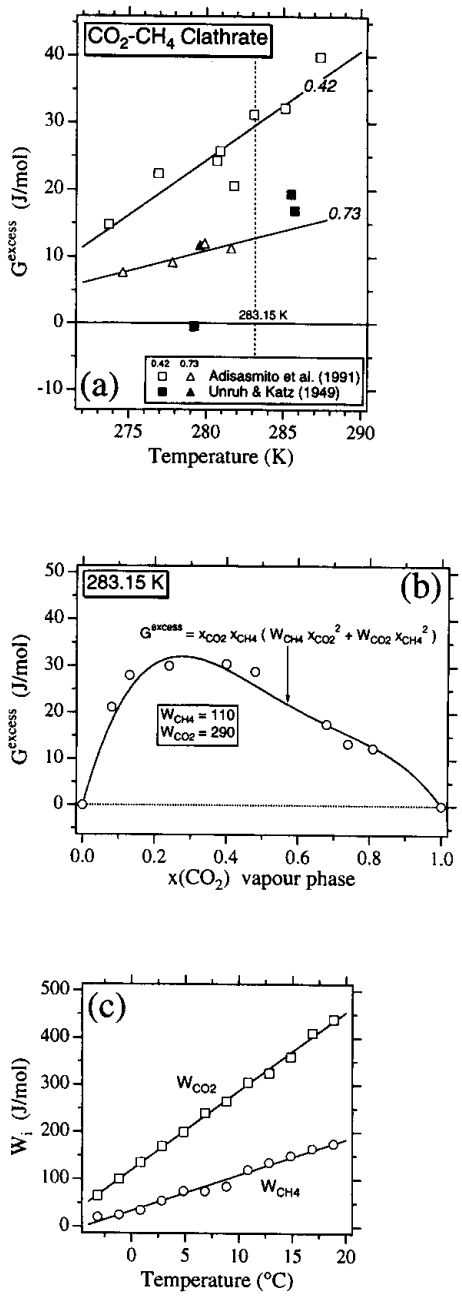

Fig. 8. (a) $T-G^{excess}$ diagram for CO_2–CH_4 gas hydrate with isopleths for 0.42 and 0.73 mole fraction CO_2; (b) $X-G^{excess}$ diagram for CO_2–CH_4 gas hydrate at 283.15 K; and (c) $T-W_G$ diagram with the interchange energies for CO_2 and CH_4 in CO_2–CH_4 gas hydrate.

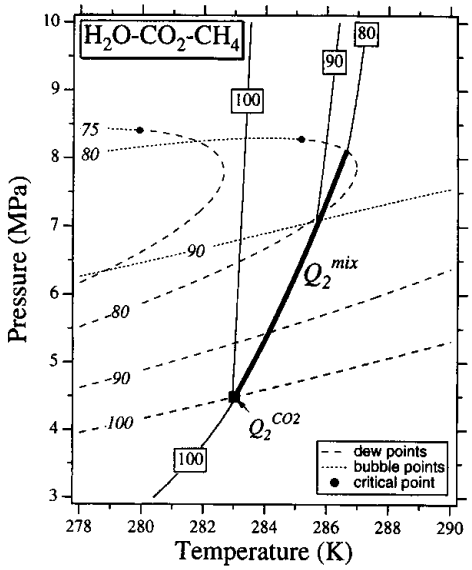

Fig. 9. $T-P$ diagram for CO_2–CH_4 mixed gas hydrate near Q_2 melting conditions. Curved dashed lines illustrate the position of immiscibility for CO_2–CH_4 fluids, numbers are mol% CO_2. Thin solid lines are clathrate stability curves for several selected vapour compositions (squared numbers are mol% CO_2). The thick solid line is the line segment which contains all possible clathrate melting at Q_2 conditions.

CH_4 the clathrate melting curve no longer intersects the immiscibility curve, and Q_2 disappears. For higher mole fractions of CH_4 the clathrate phase melts in the presence of a supercritical fluid. For 90 mol% CO_2 mixture, the gas-rich phase at the lower Q_2 point is vapour-like, while the higher Q_2 point has a liquid-like gas-rich phase. The 80 mol% CO_2 mixture has a vapour-like gas-rich phase at both the lower and upper Q_2 point (Fig. 9). The position of the critical point of this mixture is located within the clathrate stability field, while the dew-point line intersects this boundary twice.

The distribution of CO_2 and CH_4 between the clathrate phase and the fluid is illustrated in Fig. 10. Within a small temperature range, between 283 and 293 K, this fluid system has an azeotrope. The clathrate phase in equilibrium with a CH_4-rich fluid is relatively enriched in CO_2, and a clathrate phase in equilibrium with a CO_2-rich fluid is strongly enriched in CH_4. The azeotropic point moves from CO_2-rich compositions near 283 K to CH_4-rich compositions at higher temperatures. The 284 K isotherm in Fig. 10 intersects the immiscibility field for CO_2–CH_4 fluids, which defines Q_2. The relative

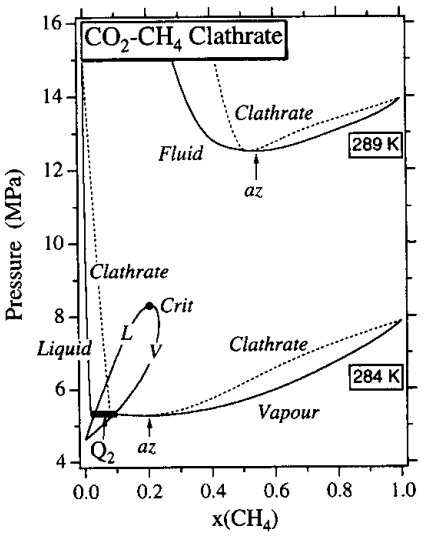

Fig. 10. P–X diagram for CO_2–CH_4 mixed gas hydrate with two isotherms (284 and 289 K). Mole fraction CH_4 is calculated on a water-free basis. L, liquid phase; V, vapour phase; Crit, critical point at 284 K, az, azeotropic point.

amount of CH_4 in the clathrate compared to CO_2 is similar to the composition of the vapour phase, while the coexisting liquid phase is slightly enriched in CO_2.

CH_4–N_2 gas hydrate

The hydrate formers CH_4 and N_2 have different clathrate structures, I and II, respectively. Therefore, mixed CH_4–N_2 gas hydrates can form both type of structures, which is mainly defined by their composition. Neither pure CH_4 nor pure N_2 gas hydrates have a Q_2 point, and clathrate melting always occurs in the presence of a supercritical fluid. The equation of state according to Duan *et al.* (1996) is selected to calculate fugacities in CH_4–N_2 mixtures. Although this equation of state was originally not used for pure CH_4 gas hydrate, it has a similar accuracy to the equation of state from Duan *et al.* (1992*a*, *b*) (see Fig. 2b).

Jhaveri & Robinson (1965) provide the sole experimental data set in this fluid system. Therefore, the estimation of excess functions must be regarded as a first approach. The difference between measured and modelled clathrate melting pressures without excess energy may exceed 30% for gas mixtures of *c.* 30 mol% CH_4, which, again, greatly exceeds the accuracy of the pure end-members. The missing energy G^{excess} in equation (19) has been calculated for each individual experimental data point (Fig. 11 and Table 14). A simple dependence on mole fraction and temperature, like that for CO_2–CH_4 gas hydrates, is not easily observed

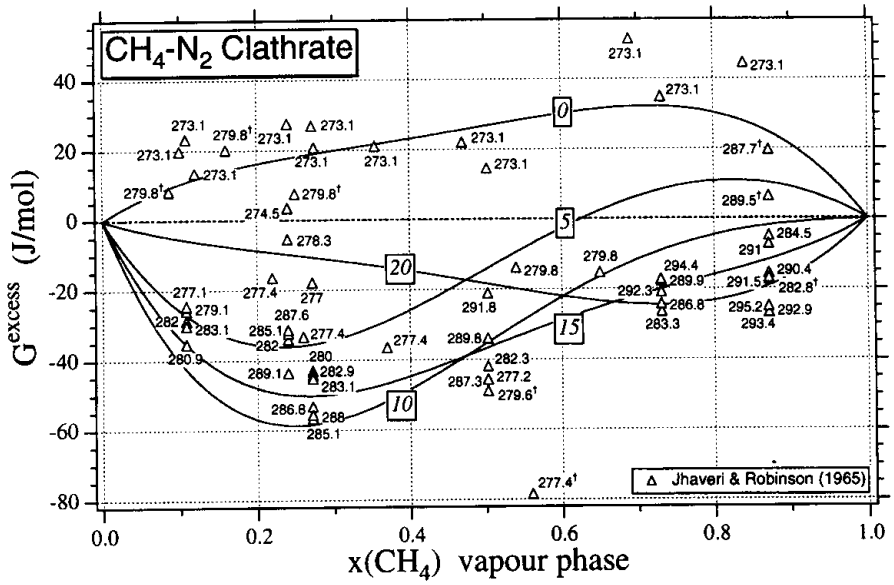

Fig. 11. G^{excess}–X diagram for CH_4–N_2 mixed gas hydrate. Numbered temperatures for individual data points are in Kelvin. Curved solid lines are modelled G^{excess} values according to equations (21) and (22) at selected temperatures (squared numbers in °C). Experimental data points marked with an † are excluded from the estimation of interchange energies W_G.

Table 14. *Measured clathrate stability conditions and calculated* G^{excess} *and mole fraction in the clathrate phase for the binary* CH_4–N_2 *gas hydrate*

Literature	Measured values				Calculated values	
	xCH_4(vap)	T (K)	P (MPa)	G^{excess} ($J\,mol^{-1}$)	xCH_4(cla)	xN_2(cla)
Jhaveri & Robinson (1965)	0.873	282.76	7.40	−17.46	0.138	0.005
		284.54	9.31	−4.94	0.139	0.005
		287.71	14.52	19.61	0.139	0.006
		289.48	17.11	6.43	0.139	0.006
		290.37	17.49	−15.67	0.139	0.006
		290.98	19.53	−7.27	0.139	0.006
		291.48	19.99	−16.99	0.139	0.006
		292.87	22.94	−26.83	0.139	0.007
		293.43	24.66	−26.73	0.138	0.007
		295.21	31.31	−25.02	0.138	0.007
	0.731	273.15	3.90	34.86	0.132	0.009
		283.32	8.95	−26.49	0.132	0.011
		286.82	13.22	−24.37	0.132	0.012
		289.93	19.55	−17.91	0.131	0.014
		292.32	25.99	−20.91	0.130	0.015
		294.43	34.34	−17.31	0.129	0.017
	0.5025	273.15	4.96	14.57	0.119	0.022
		277.21	6.13	−45.65	0.118	0.023
		279.65	7.77	−48.93	0.118	0.024
		282.32	10.49	−41.90	0.117	0.026
		287.32	17.90	−45.70	0.115	0.029
		289.82	24.99	−33.93	0.114	0.031
		291.82	33.19	−21.18	0.112	0.033
	0.272	273.15	7.96	26.93	0.094	0.048
		277.04	10.16	−17.92	0.092	0.050
		279.98	12.64	−43.06	0.091	0.051
		282.87	17.04	−44.34	0.089	0.054
		283.15	17.50	−45.28	0.089	0.054
		285.09	20.72	−56.69	0.088	0.056
		286.76	25.14	−53.21	0.087	0.057
		287.98	28..49	−55.58	0.086	0.058
	0.24	273.15	8.62	27.60	0.088	0.053
		274.54	9.15	3.51	0.088	0.054
		278.26	12.96	−5.42	0.086	0.056
		282.04	17.44	−33.93	0.084	0.059
		285.09	24.34	−32.27	0.082	0.062
		287.59	31.99	−31.31	0.080	0.065
		289.09	35.96	−43.60	0.079	0.066
	0.108	273.15	12.55	23.22	0.055	0.087
		277.15	15.86	−25.78	0.053	0.089
		279.09	19.39	−24.44	0.052	0.091
		280.93	22.52	−35.28	0.051	0.092
		282.04	25.82	−28.60	0.050	0.093
		283.15	28.79	−30.10	0.050	0.094
Jhaveri & Robinson (1965)	0.840	273.15	3.56	44.47	0.136	0.005
	0.690		4.31	51.36	0.130	0.011
	0.470		5.35	22.00	0.116	0.025
	0.355		6.55	21.00	0.105	0.036
	0.275		7.75	20.759	0.094	0.047
	0.185		10.64	46.98	0.077	0.065
	0.120		11.65	13.48	0.059	0.083
	0.100		12.77	19.81	0.052	0.090
	0.075		13.32	9.56	0.031	0.104
	0.060		14.59	22.92	0.026	0.111
	0.560	277.43	5.20	−78.49	0.122	0.019
	0.370		8.11	−36.43	0.106	0.036
	0.260		10.34	−33.23	0.090	0.052
	0.220		12.06	−16.52	0.083	0.059
	0.650	279.82	7.14	−15.39	0.128	0.014
	0.540		8.37	−13.91	0.121	0.022
	0.250		15.55	7.57	0.087	0.056
	0.160		20.67	20.14	0.067	0.077
	0.086		25.23	8.32	0.043	0.101

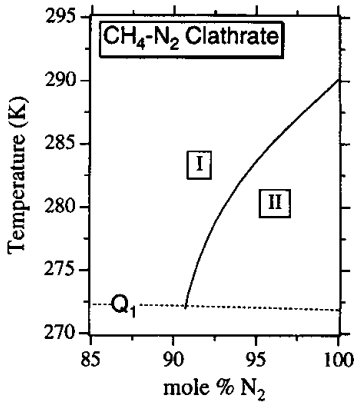

Fig. 12. T–X diagram for CH_4–N_2 mixed gas hydrate with the boundary between clathrate Structure I and II. Mole fraction N_2 is calculated on a water-free basis.

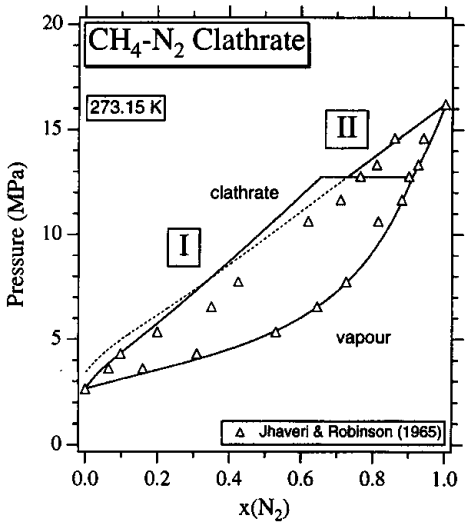

Fig. 13. P–X diagram for CH_4–N_2 mixed gas hydrate at 273.15 K. Mole fraction N_2 is calculated on a water-free basis. Iand II are the stability fields for clathrate Structure I and Structure II, respectively.

from Fig. 11. Some experimental data do not follow the general trend in temperature dependence at selected compositions. However, relatively simple equations for temperature and mole fraction dependency of G^{excess} and interchange energies (Table 12) are estimated after careful analysis of Fig. 10. The non-ideality switches from positive excess energies at 273 K to negative values at higher temperatures (>278 K). At temperatures higher than 283 K, G^{excess} switches back in the direction of positive values only for CH_4-rich compositions, while N_2-rich compositions continue to decrease in value. The asymmetry changes from most intensively non-ideal for CH_4-rich compositions, similar to CO_2–CH_4 gas hydrates, to N_2-rich compositions at higher temperatures. In general, the calculated chemical potential for clathrate Structure II exceeds that for Structure I clathrates for all experimental data in Fig. 11 and Table 14. Consequently, clathrate Structure I is the most stable configuration, even for N_2-rich compositions. The stability of clathrate Structure II is limited to a small range at high N_2 mole fractions (>0.91) and relatively low temperature (Fig. 12).

The distribution of N_2 and CH_4 between the clathrate phase and the vapour phase at 273.15 K is illustrated in Fig. 13. The clathrate phase is systematically enriched in CH_4. Theoretical considerations already suggest that denser phases are enriched in less volatile components which have higher critical points. Modelled compositions of the vapour phase at selected pressures are consistent with the experimental data from Jhaveri & Robinson (1965). However, the coexisting composition of the clathrate phase is very dissimilar, which may result from large uncertainties in measured values. Experimental data which are located in the modelled stability field of clathrate Structure I are more likely to correspond to a modelled clathrate Structure II (Fig. 13). Small difference in chemical potential between Structure I and Structure II may ease the presence of a metastable phase during experiments. This example illustrates the advantage of presenting the clathrate phase G^{excess} as a function of the vapour phase composition, which is experimentally verifiable.

CH_4–C_2H_6 gas hydrate

The CH_4–C_2H_6 gas mixture forms clathrate Structure I over the total compositional range. Fugacities in gas mixtures are calculated using the equation of state according to Lee & Kesler (1975). This equation accurately reproduces fugacity coefficients for pure CH_4, C_2H_6 and mixtures up to 300 K (Fig. 2b and d).

Experimental data from Deaton & Frost (1946), McLeod & Campbell (1961) and Holder & Grigoriou (1980) are compared to model predictions. Again, the model without a G^{excess} function is unable to reproduce stability conditions of the mixed gas hydrate. Table 15 and Fig. 14 illustrate the amount of missing energy in the model to obtain a perfect fit to experimental data. Although three independent data

Table 15. *Measured clathrate stability conditions and calculated* G^{excess} *and mole fractions in the clathrate phase for binary* CH_4–C_2H_6 *gas hydrate*

Literature	Measured values				Calculated values	
	xCH_4(vap)	T (K)	P (MPa)	G^{excess} (J mol^{-1})	xCH_4(cla)	xC_2H_6(cla)
Deaton & Frost (1946)	0.988	274.8	2.86	−7.45	0.131	0.009
	0.988	277.6	3.81	−3.72	0.132	0.009
	0.988	280.4	5.09	−0.47	0.134	0.008
	0.978	274.8	2.36	−53.46	0.122	0.017
	0.978	277.6	3.23	−41.57	0.125	0.016
	0.978	280.4	4.41	−30.92	0.127	0.015
	0.978	282.6	5.67	−24.78	0.129	0.014
	0.978	283.1	6.09	−20.94	0.129	0.013
	0.971	274.8	2.16	−72.33	0.117	0.021
	0.971	277.6	2.96	−59.24	0.120	0.020
	0.971	280.4	4.03	−49.57	0.122	0.019
	0.950	274.8	1.84	−92.89	0.104	0.0329
	0.950	277.6	2.53	−79.97	0.107	0.032
	0.950	280.4	3.45	−71.38	0.110	0.030
	0.950	283.1	4.77	−60.53	0.113	0.028
	0.904	274.8	1.52	−95.61	0.084	0.051
	0.904	277.6	2.10	−84.38	0.088	0.050
	0.904	280.4	2.89	−73.77	0.091	0.048
	0.904	283.1	3.96	−67.13	0.094	0.046
	0.534	274.8	0.94	−14.54	0.032	0.097
	0.564	277.6	1.29	−11.88	0.035	0.096
	0.564	280.4	1.76	−10.47	0.038	0.095
	0.564	283.1	2.43	−6.71	0.041	0.094
McLeod & Campbell (1961)	0.944	302.0	68.43	24.61	0.134	0.013
	0.944	301.1	62.23	22.11	0.134	0.013
	0.944	299.0	48.23	16.52	0.133	0.013
	0.944	296.5	34.44	9.55	0.132	0.014
	0.945	293.6	24.24	20.58	0.130	0.016
	0.945	289.6	13.89	21.22	0.124	0.020
	0.945	287.9	10.45	8.29	0.121	0.023
	0.946	284.9	6.93	−3.83	0.116	0.027
	0.807	304.0	68.57	−0.76	0.108	0.038
	0.807	303.1	61.95	−2.53	0.109	0.038
	0.807	301.3	48.64	−15.28	0.108	0.038
	0.807	299.0	35.61	−19.68	0.107	0.039
	0.808	296.4	23.48	−26.19	0.103	0.042
	0.808	293.3	13.89	−27.17	0.094	0.050
	0.808	291.7	10.45	−29.44	0.088	0.055
	0.808	288.8	7.00	−23.43	0.081	0.061
Holder & Grigoriou (1980)	0.983	283.9	1.81	−453.53	0.122	0.012
	0.983	285.7	2.31	−431.05	0.124	0.011
	0.983	286.6	2.71	−406.97	0.125	0.011
	0.983	287.8	3.08	−403.81	0.126	0.011
	0.952	279.4	0.99	−455.32	0.098	0.031
	0.952	281.5	1.34	−425.97	0.101	0.030
	0.952	283.3	1.71	−405.25	0.104	0.029
	0.952	285.3	2.17	−392.90	0.106	0.029
	0.952	286.4	2.51	−381.28	0.108	0.028
	0.952	287.6	2.99	−363.40	0.110	0.028
	0.822	281.6	1.42	−269.34	0.064	0.069
	0.822	283.3	1.77	−255.824	0.066	0.098
	0.822	284.8	2.14	−245.67	0.068	0.067
	0.822	286.2	2.66	−233.81	0.071	0.066
	0.822	287.0	2.96	−217.32	0.072	0.065

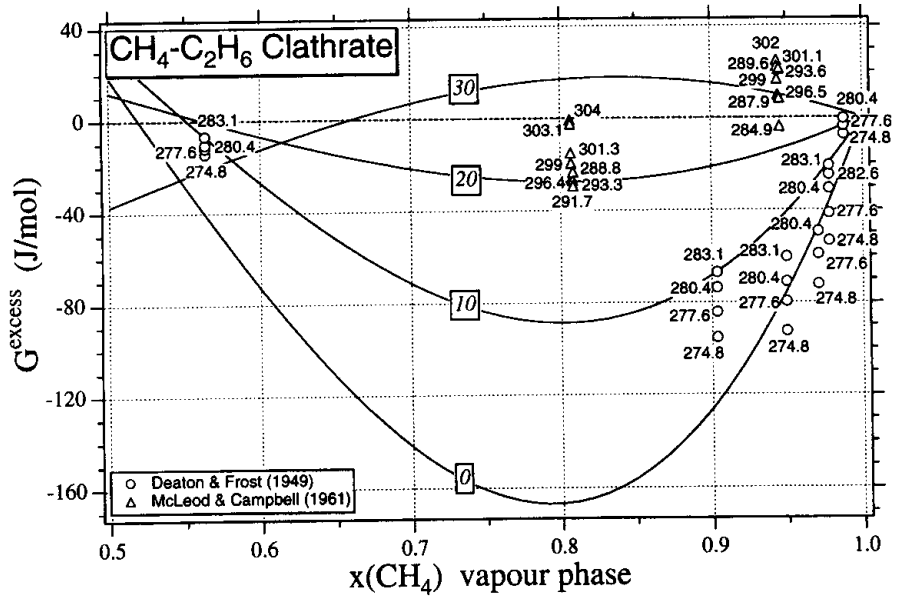

Fig. 14. $G^{excess}-X$ diagram for $CH_4-C_2H_6$ mixed gas hydrate. Numbered temperatures for individual data points are in Kelvin. Curved solid lines are modelled G^{excess} values according to equations (21) and (22) at selected temperatures (squared numbers in °C).

sets are available, Holder & Grigoriou (1980) present data which are completely inconsistent with the other data sets. For example, clathrate melting pressure for a 95 mol% CH_4 mixture at 283.2 K is 4.77 MPa according to Deaton & Frost (1946), while Holder & Grigoriou (1980) have measured it at 1.71 MPa. In addition, the extremely high calculated G^{excess} values from their data are regarded as unrealistic. Therefore, experimental data from Holder & Grigoriou (1980) are excluded from the estimation of G^{excess} and interchange energies W_G. Figure 14 illustrates a strong asymmetry with high negative G^{excess} values for about 80 mol% CH_4 and relatively low temperatures. All data are consistent with a general trend towards positive values for increasing temperatures. Unfortunately, experimental data are not available for C_2H_6-rich fluids (>50 mol%), but the continuation of the asymmetry for CH_4-rich compositions suggests a knot at about 50 mol% and strong positive G^{excess} values at relatively low temperatures.

CO_2–N_2 gas hydrate

Experimental data are not available for this fluid system. Therefore, the excess Gibbs free energy function for CO_2–N_2 gas hydrates cannot be calculated. In a first approximation it is assumed that both interchange energies for CO_2 and N_2 are zero. However, thermodynamic considerations on the position of Q_2 for CO_2-rich gas mixtures (>75 mol%) suggest the existence of excess energy in this fluid system. Similar to the CO_2–CH_4 system (Fig. 9), a quadruple point Q_2 for pure CO_2 gas hydrate is transformed into a limited line if small amounts of N_2 are added to the fluid system (Fig. 15). The lower Q_2 point for a mixture of 90 mol% CO_2 in Fig. 15 is defined by the intersection of the dew-point line and the clathrate melting curve in equilibrium with a vapour-like CO_2-rich phase. Likewise, the upper Q_2 point is defined by the intersection of the bubble-point line and the clathrate melting curve in equilibrium with a liquid-like CO_2-rich phase. However, the coexisting vapour-like CO_2-rich phase at this point does not give an equal intersection point (Fig. 15). This gap can be closed if an G^{excess} value of 60 J mol^{-1} is used.

Computer programmes

Calculation of clathrate stability conditions in this study have been performed with the computer code CLATHRATE in C++ developed by Bakker (1997). The package of programs was developed for fluid inclusion research,

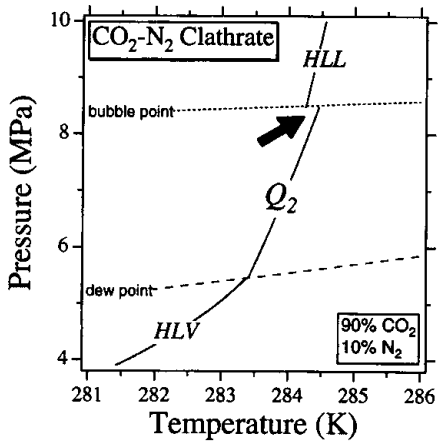

Fig. 15. T–P diagram for CO_2–N_2 gas hydrate near Q_2 conditions. The fluid has 90 mol% CO_2 and 10 mol% N_2. HLV and HLL are the clathrate melting curves in equilibrium with a vapour-like gas mixture and a liquid-like gas mixture, respectively. The arrow indicates the discontinuity in the clathrate melting curve at the bubble point.

where clathrate melting temperatures are frequently measured. The package is extended with the program CURVES, which is able to calculate clathrate melting curves for a chosen fluid composition, including salinities, and can which calculate clathrate melting pressure at a selected temperature or the inverse. Furthermore, the programs calculate the composition of the clathrate phase at a selected temperature and pressure, and the composition of each phase that is present during clathrate melting. The program can run on an IBM (compatible) computer and is readily available on request.

Conclusions

Using the most accurate estimations for fugacities, gas solubilities in H_2O and thermodynamic constants for the clathrate, liquid and vapour phase, optimum Kihara parameters σ and ε for gas–H_2O interactions are obtained for pure CO_2, CH_4, N_2, and C_2H_6 gas hydrates. A large amount of experimental data from independent sources for the fitting procedure are necessary to obtain a true best-fit. The postulates from the original clathrate stability model from van der Waals & Platteeuw (1959) are not violated in this optimization procedure. These Kihara parameters differ from previous estimations found in the literature, which can be directly related to the use of an insufficient amount of data. Experimental data for mixed gas hydrates can only be reproduced accurately after the introduction of an excess Gibbs free energy function, which must have resulted from an interaction between cavities with different filling molecules. A modified Margules equation describes the composition and temperature dependence of the excess energy for CO_2–CH_4, CH_4–N_2, and CH_4–C_2H_6 gas hydrates.

This work is financially supported by the Deutsche Forschungsgemeinschaft: Graduiertenkollegs 'Wirkung fluider Phasen auf Locker- und Festgesteine'.

References

ADISASMITO, S., FRANK, R. J. & SLOAN, E. D. Jr. 1991. Hydrates of carbon dioxide and methane mixtures. *Journal of Chemical Engineering Data*, **36**, 68–71.

ANDERSON, F. E. & PRAUSNITZ, J. M. 1986. Inhibition of gas hydrates by methanol. *American Institute of Chemical Engineering Journal*, **32**, 1321–1333.

ANGELL, C. A., SHUPPERT, J. & TUCKER, J.C. 1973. Anomalous properties of supercooled water. Heat capacity, expansivity, and proton magnetic resonance chemical shift from 0 to −38°. *Journal of Physical Chemistry*, **77**, 3092–3099.

ANGUS, S., DE REUCK, K. M. & ARMSTRONG, B. 1979. *International Thermodynamic Tables of the Fluid State: 6. Nitrogen*. Pergamon, Oxford.

AVLONITIS, D. 1988. *Multiple Equilibria in Oil-water Hydrate Forming Systems*. MSc thesis, Heriot-Watt University, UK.

—— 1994. The determination of Kihara potential parameters from gas hydrate data. *Chemical Engineering Science*, **49**, 1161–1173.

BAKKER, R. J. 1997. Clathrates: computer programmes to calculate fluid inclusion V–X properties using clathrate melting temperatures. *Computers & Geosciences*, **23**, 1–18.

——, DUBESSY, J. & CATHELINEAU, M. 1996. Improvements in clathrate modeling. I: The H_2O–CO_2 system with various salts. *Geochimica et Cosmochimica Acta*, **60**, 1657–1681.

BENEDICT, M., WEBB, G. B. & RUBIN, L. C. 1949. An empirical equation for thermodynamic properties of light hydrocarbons and their mixtures I. Methane, ethane, propane and n-butane. *Journal of Chemical Physics*, **8**, 334–345.

BENSON, B. B. & KRAUS D., JR. 1976. Empirical laws for dilute aqueous solutions of nonpolar gases. *Journal of Chemical Physics*, **64**, 689–709.

BOZZO, A. T., CHEN, H.-S., KASS, J. R. & BARDUHN, A. J. 1975. The properties of the hydrates of chlorine and carbon dioxide. *Desalination*, **16**, 303–320.

CARNAHAN, N. F. & STARLING K. E. 1969. Equation of state for non-attracting rigid spheres. *Journal of Chemical Physics*, **51**, 635–636.

CARROLL, J. J. & MATHER, A. E. 1992. The system

carbon dioxide–water and the Krichevsky–Kasarnovsky equation. *Journal of Solution Chemistry*, **21**, 607–621.

——, SLUPSKY, J. D. & MATHER, A. E. 1991. The solubility of carbon dioxide in water at low pressure. *Journal of Physical Chemistry Reference Data*, **20**, 1201–1209.

CHUEH, P. L. & PRAUSNITZ, J. M. 1967. Vapor–liquid equilibria at high pressures. Vapor-phase fugacity coefficients in nonpolar and quantum–gas mixtures. *Industrial and Engineering Chemistry Fundamentals*, **6**, 492–498.

CULBERSON, O. L. & MCKETTA, J. J., JR. 1951. Phase equilibria in hydrocarbon–water systems III: The solubility of methane in water at pressures to 10,000 psia. *Petroleum Transactions, American Institute for Mechanical Engineers*, **192**, 223–226.

DAVIDSON D. W., GOUGH, S. R., HANDA, Y. P., RATCLIFFE, C. I., RIPMEESTER, J. A. & TSE, J. S. 1987. Some structural studies of clathrate hydrates. *Journal de Physique C1*, **3**, 537–542.

DEATON, W. M. & FROST, E. M., JR. 1946. *Gas Hydrates and their Relation to Operation of Natural-gas Pipe Lines*. United States Bureau of Minerals Monograph **8**, 1–108.

DEBYE, P. & HÜCKEL, E. 1923. Zur Theorie der Electrolyte I: Gefrierpunktserniederung und verwandte Erscheinungen. *Physikalisch Zeitschrift*, **24**, 185–206.

DE ROO, J. L., PETERS, C. J., LICHTENTHALER, R. N. & DIEPEN, G. A. M. 1983. Occurence of methane hydrate in saturated and unsaturated solutions of sodium chloride and water in dependence of temperature and pressure. *American Institute of Chemical Engineering Journal*, **29**, 651–657.

DHARMAWARDHAMA, P. B., PARRISH, W. R. & SLOAN, E. D. JR. 1980. Experimental thermodynamic parameters for the prediction of natural gas hydrate dissociation conditions. *Industrial Engineering and Chemical Fundamentals*, **19**, 410–414.

DHOLABHAI, P. D., KALOGERAKIS, N. & BISHNOI, P. R. 1993. Equilibrium conditions for carbon dioxide hydrate formation in aqueous electrolyte solutions. *Journal of Chemical Engineering Data*, **38**, 650–654.

DICKENS, G. R. & QUINBY-HUNT, M. S. 1994. Methane hydrate stability in seawater. *Geophysical Research Letters*, **21**, 2115–2118.

DUAN, Z., MØLLER, N. & WEARE, J. H. 1992*a*. An equation of state for the CH_4–CO_2–H_2O system: I. Pure systems from 0 to 1000°C and 0 to 8000 bar. *Geochimica et Cosmochimica Acta*, **56**, 2605–2617.

——, —— & —— 1992*b*. An equation of state for the CH_4–CO_2–H_2O system: II. Mixtures from 50 to 1000°C and 0 to 1000 bar. *Geochimica et Cosmochimica Acta*, **56**, 2619–2631.

——, —— & —— 1996. A general equation of state for supercritical fluid mixtures and molecular dynamics simulation of mixture PVTX properties. *Geochimica et Cosmochimica Acta*, **60**, 1209–1216.

DUBESSY, J., THIÉRY, R. & CANALS, M. 1992. Modeling of phase equilibria involving mixed gas clathrates: application to the determination of molar volume of the vapour phase and salinity of aqueous solution in fluid inclusions. *European Journal of Mineralogy*, **4**, 873–884.

ENGLEZOS, P. & BISHNOI, P. R. 1988. Prediction of gas hydrate formation conditions in aqueous electrolyte solutions. *American Institute for Chemical Engineering Journal*, **34**, 1718–1721.

—— & —— 1991. Experimental study on the equilibrium ethane hydrate formation conditions in aqueous electrolyte solutions. *Industrial and Engineering Chemistry Research*, **30**, 1655–1659.

—— & HALL, S. 1994. Phase equilibrium data on carbon dioxide hydrate in the presence of electrolytes, water soluble polymers and montmorillonite. *Canadian Journal of Chemical Engineering*, **72**, 887–893.

FLOWERS, G. C. 1979. Correction of Holloway's (1977) adaption of the modified Redlich-Kwong equation of state for calculation of the fugacities of molecular species in supercritical fluids of geologic interest. *Contributions to Mineralogy and Petrology*, **69**, 315–319.

FRANKS, F. 1972. *Water, A Comprehensive Treatise*. Plenum, New York.

FRIEND, D. G., INGHAM, H. & ELY, J. F. 1991. Thermophysical properties of ethane. *Journal of Physical Chemistry Reference Data*, **20**, 275–347.

GALLOWAY, T. J., RUSKA, W., CHAPPELEAR, P. S. & KOBAYASHI, R. 1970. Experimental measurements of hydrate numbers for methane and ethane and comparison with theoretical values. *Industrial Engineering and Chemistry Fundamentals*, **9**, 237–243.

GIAUQUE, W. F. & STOUT, J. W. 1936. The entropy of water and the third law of thermodynamics. Heat capacity of ice from 15 to 273 K. *Journal of the American Chemical Society*, **58**, 1144–1150.

HAAR, L., GALLAGHER, J. S. & KELL, G. S. 1984. *NBS/NRC Steam Tables*. Hemisphere, Washington, DC.

HILL, P. G. 1990. A unified fundamental equation for the termodynamic properties of H_2O. *Journal of Physics and Chemistry Reference Data*, **19**, 1233–1274.

HOLDER, G. D. & GRIGORIOU, G. C. 1980. Hydrate dissociation pressures of (methane + ethane + water). Existence of a locus minimum pressure. *Journal of Chemical Thermodynamics*, **A150**, 1093–1104.

—— & HAND, J. H. 1982. Multiple-phase equilibria in hydrates from methane, ethane, propane, and water mixtures. *American Institute for Chemical Engineering Journal*, **28**, 440–447.

——, CORBIN, G. & PAPADOPOULOS, K. D. 1980. Thermodynamic and molecular properties of gas hydrates from mixtures containing methane, argon, and krypton. *Industrial Engineering and Chemistry Fundamentals*, **19**, 282–286.

——, ZETTS, S. P. & PRADHAN, N. 1988. Phase behaviour in systems containing clathrate hydrates, a review. *Reviews in Chemical Engineering*, **5**, 1–70.

HOLLOWAY, J. R. 1977. Fugacity and activity of molecular species in supercritical fluids. *In:*

FRASER, D. G. (ed.) *Thermodynamics in Geology*, 161–182.

—— 1981. Compositions and volumes of supercritical fluids in the earth's crust. *In*: HOLLISTER, L. S. & CRAWFORD, M. L. (eds) *Short Course in Fluid Inclusions: Application to Petrology*, 13–38.

JHAVERI, J. & ROBINSON, D. B. 1965. Hydrates in the methane-nitrogen system. *Canadian Journal of Chemical Engineering*, **43**, 75–78.

JOHN, V. T. & HOLDER, G. D. 1981. Langmuir constants for spherical and linear molecules in clathrate hydrates. Validity of the cell theory. *Journal of Physical Chemistry*, **89**, 3279–3285.

——, PAPADOPOULOS, K. D. & HOLDER, G. D. 1985. A generalized model for predicting equilibrium conditions for gas hydrates. *American Institute of Chemical Engineering Journal*, **31**, 252–259.

JONES, J. E. 1924. On the determination of molecular fields II: From the equation of state of a gas. *Proceedings of the Royal Society of London*, **A106**, 463–477.

KELL, G. S. 1967. Precise representation of volumetric properties of water at one atmosphere. *Journal of Chemical Engineering Data*, **12**, 66–69.

—— & WHALLEY, E. 1965. The PVT properties of water. I. Liquid water in the temperature range 0 to 150°C and at pressures up to 1 kb. *Philosophical Transactions of the Royal Society of London*, **258A**, 565–614.

KIHARA, T. 1953. Virial coefficients and models of molecules in gases. *Reviews in Modern Physics*, **25**, 831–843.

KOBAYASHI, R. & KATZ, D. L. 1949. Methane hydrate at high pressures. *Petroleum Transactions, American Institute for Mechanical Engineers*, **1**, 66–70.

KRICHEVSKY, I. R. & KASARNOWSKY, J. S. 1935. Thermodynamical calculations of solubilities of nitrogen and hydrogen in water at high pressures. *Journal of the American Chemical Society*, **57**, 2168–2172.

LANGMUIR, I. 1918. The adsorption of gases on plane surfaces of glass, mica and platinum. *Journal of the American Chemical Society*, **40**, 1361–1403.

LARSON, S. D. 1955. *Phase Studies of Two-component Carbon Dioxide–Water System Involving the Carbon Dioxide Hydrate*. PhD thesis, University of Illinois.

LEE, B. I. & KESLER, M. G. 1975. A generalized thermodynamic correlation based on three-parameter corresponding states. *American Institute of Chemical Engineering Journal*, **21**, 510–527.

LENNARD-JONES, J. E. & DEVONSHIRE, A. F. 1937. Critical phenomena in gases I. *Proceedings of the Royal Society of London*, **163**, 53–70.

—— & —— 1938. Critical phenomena in gases. II: Vapour pressures and boiling points. *Proceedings of the Royal Society of London*, **165**, 1–11.

LUNDGAARD, L. & MOLLERUP, J. 1991. The influence of gas phase fugacity and solubility on correlations of gas-hydrate formation pressure. *Fluid Phase Equilibria*, **70**, 199–213.

—— & —— 1992. Calculation of phase diagrams of gas-hydrates. *Fluid Phase Equilibria*, **76**, 141–149.

MARGULES, M. 1895. Über die Zusammensetzung der gesättigten Dämpfe von Mischungen. *Sitzungberichte der Wiener Akademie*, **104**, 1243–1278.

MARSHALL, D. R., SAITO, S. & KOBAYASHI, R. (1964) Hydrates at high pressure, part I: methane–water, argon–water, and nitrogen–water system. *American Institute of Chemical Engineering Journal*, **10**, 202–205.

MCKOY, V. & SINANOGLU, O. 1963. Theory of dissociation pressures of some gas hydrates. *Journal of Chemical Physics*, **38**, 2946–2956.

MCLEOD, H. O. & CAMPBELL, J. M. 1961. Natural gas hydrates at pressures to 10,000 psia. *Journal of Petroleum Technology*, **222**, 590–594.

MOORE, J. C., BATTINO, R., RETTICH, T. R., HANDA, Y. P. & WILHELM, E. 1982. Partial molar volumes of 'gases' at infinite dolution in water at 298.15 K. *Journal of Chemical Engineering Science*, **27**, 22–24.

MUNCK, J., SKJOLD-JORGENSEN, S. & RASMUSSEN, P. 1988. Computations of the formation of gas hydrates. *Chemical Engineering Data*, **27**, 22–24.

NG, H. J. & ROBINSON, D. B. 1976. The measurement and prediction of hydrate formation in liquid hydrocarbon–water systems. *Industrial and Engineering Chemistry Fundamentals*, **15**, 293–298.

—— & —— 1985. Hydrate formation in systems containing methane, ethane, propane, carbon dioxide or hydrogen sulphide in the presence of methanol. *Fluid Phase Equilibria*, **21**, 145–155.

OSBORNE, N. S., STIMSOM, H. F. & GINNINGS, D. C. 1939. Measurements of heat capacity and heat of vaporization of water in the range of 0° to 100°C. *Journal of Research National Bureau of Standards*, **23**, 145–155.

PARRISH, W. R. & PRAUSNITZ, J. M. 1972. Dissociation pressure of gas hydrates formed by gas mixtures. *Industrial and Engineering Chemistry, Processes, Design, and Development*, **11**, 26–35.

PITZER, K. S. 1992. Ion interaction approach: theory and data correlation. *In*: PITZER, K. S. (ed.) *Activity Coefficient in Electrolyte Solutions*. CRC, Boca Raton, FL, 76–153.

PLATTEEUW, J. C. & VAN DER WAALS, J. H. 1958. Thermodynamic properties of gas hydrates. *Molecular Physics*, **1**, 91–96.

PRAUSNITZ, J. M., LICHTENTHALER, R. N. & DE AZEVEDO, E.G. 1986. *Molecular Thermodynamics of Fluid-phase Equilibria*. Prentice-Hall, Englewood Cliffs, NJ.

REAMER, H. H., SELLECK, F. T. & SAGE, B. H. 1952. Some properties of mixed paraffinic and olefinic hydrates. *Petroleum Transactions, American Institute for Mechanical Engineers*, **195**, 197–205.

REDLICH, O. & KWONG, J. N. S. 1949. On the thermodynamics of solutions V: an equation of state. Fugacities of gaseous solutions. *Chemical Reviews*, **44**, 233–244.

RETTICH, T. R., HANDA, Y. P, BATTINO, R. & WILHELM, E. 1981. Solubility of gases in liquids 13. High-precision determination of Henry's constants for methane and ethane in liquid water at 275 to 328 K. *Journal of Physical Chemistry*, **85**, 3230–3237.

RIGBY M. & PRAUSNITZ, J. M. 1968. Solubility of water

in compressed nitrogen, argon, and methane. *Journal of Physical Chemistry*, **72**, 330–334.

ROBERTS, O. L., BROWNSCOMBE, E. R. & HOWE, L. S. 1940. Methane and ethane hydrates. *Oil & Gas Journal*, **39**, 37–42.

ROBINSON, D. B. & METHA, B. R. 1971. Hydrates in the propane–carbon dioxide–water system. *Journal of Canadian Petroleum Technology*, **10**, 33–35.

ROEDDER, E. 1963. Studies of fluid inclusions. II: Freezing data and their interpretation. *Economical Geology*, **58**, 167–211.

SAITO, S., MARSHALL, D. R. & KOBAYASHI, R. 1964. Hydrates at high pressures, part II: Application of statistical mechanics to the study of the hydrates of methane, argon, and nitrogen. *American Institute of Chemical Engineering Journal*, **10**, 734–740.

SETZMANN, U. & WAGNER, W. 1991. A new equation of state and tables of thermodynamic properties for methane covering the range from the melting line to 625 K at pressure up to 1000 MPa. *Journal of Physical Chemistry Reference Data*, **20**, 1061–115.

SLOAN, E. D., JR. 1990. *Clathrate Hydrates of Natural Gases*. Chemical Industries, Volume 39., Marcel Dekker, New York.

SOAVE, G. 1972. Equilibrium constants from a modified Redlich–Kwong equation of state. *Chemical Engineering Science*, **27**, 1197–1203.

SPAN, R. & WAGNER, W. 1996. A new equation of state for carbon dioxide covering the fluid region from the triple-point temperature to 1100 K at pressures up to 800 MPa. *Journal of Physical Chemistry Reference Data*, **25**, 1509–1596.

TAKENOUCHI, S. & KENNEDY, G. C. 1965. Dissociation of the phase CO_2–$5.75H_2O$. *Journal of Geology*, **73**, 383–390.

TEE, L. S., GOTOH, S. & STEWARD, W. E. 1966. Molecular parameters for normal fluids, Kihara potential with spherical core. *Industrial and Engineering Chemistry Fundamentals*, **5**, 363–367.

THIÉRY, R., VAN DEN KERKHOF, A. M. & DUBESSY, J. 1994. VX properties of CH_4–CO_2 and CO_2–N_2 fluid inclusions: modeling for $T < 31°C$ and $P < 400$ bars. *European Journal of Mineralogy*, **6**, 753–771.

THOMPSON, J. B. Jr. 1967. Thermodynamic properties of simple solutions. *In:* ABELSON, P. H. (ed.) *Researches in Geochemistry*, Volume 2. Wiley, New York, 340–361.

UNRUH, C. H. & KATZ, D. L. 1949. Gas hydrates of carbon dioxide–methane mixtures. *Journal of Petroleum Technology*, **1**, 83–86.

VAN CLEEFF, A. & DIEPEN, G. A. M. 1960. Gas hydrates of nitrogen and oxygen. *Recueil des Travaux Chiniques des Pays-Bas*, **79**, 582–586.

VAN DER WAALS, J. D. 1873. *De continuiteit van den gas- en vloeistoftoestand.* Academisch Proefschrift Leiden, Sijthof.

—— & PLATTEEUW, J. C. 1959. Clathrate solutions. *Advances in Chemical Physics*, **2**, 1–57.

VERMA, V. K., HAND, J. H., KATZ, D. L. & HOLDER, G. D. 1975. Denuding hydrocarbon liquids of natural gas constituents by hydrate formation. *Journal of Petroleum Technology*, **27**, 223–226.

VON STACKELBERG, M. & MÜLLER, H. R. 1954. Feste Gashydrate II: Structur und Raumchemie. *Zeitschrift fr Electrochemie*, **58**, 25–39.

YEROKHIN, A.M. 1993. A new method of determining CO_2 density and solution concentration in H_2O–CO_2–NaCl inclusions from the gas-hydrate melting point. *Geochemistry International*, **30**, 107–129.